

## A sustainable battery scheduling and echelon utilization framework for electric bus network with photovoltaic charging infrastructure

Liu, Xiaohan; Shang, Wen Long; Correia, Gonçalo Homem de Almeida; Liu, Zhengke; Ma, Xiaolei

**DOI**

[10.1016/j.scs.2023.105108](https://doi.org/10.1016/j.scs.2023.105108)

**Publication date**

2023

**Document Version**

Final published version

**Published in**

Sustainable Cities and Society

**Citation (APA)**

Liu, X., Shang, W. L., Correia, G. H. D. A., Liu, Z., & Ma, X. (2023). A sustainable battery scheduling and echelon utilization framework for electric bus network with photovoltaic charging infrastructure. *Sustainable Cities and Society*, 101, Article 105108. <https://doi.org/10.1016/j.scs.2023.105108>

**Important note**

To cite this publication, please use the final published version (if applicable). Please check the document version above.

**Copyright**

Other than for strictly personal use, it is not permitted to download, forward or distribute the text or part of it, without the consent of the author(s) and/or copyright holder(s), unless the work is under an open content license such as Creative Commons.

**Takedown policy**

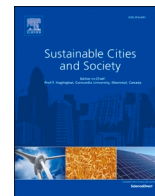
Please contact us and provide details if you believe this document breaches copyrights. We will remove access to the work immediately and investigate your claim.

***Green Open Access added to TU Delft Institutional Repository***

***'You share, we take care!' - Taverne project***

**<https://www.openaccess.nl/en/you-share-we-take-care>**

Otherwise as indicated in the copyright section: the publisher is the copyright holder of this work and the author uses the Dutch legislation to make this work public.



# A sustainable battery scheduling and echelon utilization framework for electric bus network with photovoltaic charging infrastructure

Xiaohan Liu<sup>a</sup>, Wen-Long Shang<sup>b,c,d</sup>, Gonçalo Homem de Almeida Correia<sup>e</sup>, Zhengke Liu<sup>a</sup>, Xiaolei Ma<sup>a,f,\*</sup>

<sup>a</sup> School of Transportation Science and Engineering, Beihang University, Beijing 100191, China

<sup>b</sup> Beijing Key Laboratory of Traffic Engineering, College of Metropolitan Transportation, Beijing University of Technology, Beijing, China

<sup>c</sup> School of Traffic and Transportation, Beijing Jiaotong University, Beijing, China

<sup>d</sup> Centre for Transport Studies, Imperial College London, London, United Kingdom

<sup>e</sup> Department of Transport and Planning, Delft University of Technology, the Netherlands

<sup>f</sup> Key Laboratory of Intelligent Transportation Technology and System, Ministry of Education, Beijing 100191, China

## ARTICLE INFO

### Keywords:

Public transport  
Energy storage system  
Dynamic programming  
Solar energy  
Battery capacity degradation

## ABSTRACT

Battery capacity degradation in battery electric buses (BEBs) poses a significant operational challenge for transit agencies. This study presents a sustainable battery scheduling and echelon utilization framework considering battery capacity fading and charging infrastructure integrated with solar photovoltaic (PV) and energy storage systems. The framework aims to minimize the sum of bus charging, battery replacement, and carbon emission costs during the BEB lifespan. We first present a power battery replacement problem for a single bus fleet, then extend it to a joint power battery replacement and fleet-depot matching problem. Finally, we propose a power battery replacement and fleet-depot problem by introducing solar PV and energy storage systems. Dynamic programming, Lagrange relaxation, and a two-step approach are adopted to solve the three problems. A case study involving six bus depots in Beijing demonstrates that optimal battery replacement schedules can significantly lower charging costs. Moreover, integrating solar PV and energy storage is shown to considerably reduce both charging costs and carbon emissions.

## 1. Introduction

Transportation carries a significant burden in advancing towards the Net Zero Goal by 2050. Among various sectors within transportation, road transport is the most significant contributor to carbon emissions (International Energy Agency, 2022). Notably, private cars are responsible for 38% of these emissions within the road sector (International Energy Agency, 2023). In contrast, buses have emerged as a more environmentally sustainable mode of transport, mainly due to their high passenger capacity (Schäfer & Yeh, 2020). Moreover, rapid advancements in transportation electrification and automation (Liu et al., 2021; Yan et al., 2022; Cui et al., 2023), especially in electric vehicles (Koten & Bilal, 2018; Koten, 2018), are driving notable improvements in both carbon emission reduction and safety across the transportation sectors.

### 1.1. Background

In the past decade, bus fleet electrification (BFE) has become a worldwide consensus to improve air quality and combat climate change (Lopez De Briñas Gorosabel et al., 2022). However, this transition faces two traditional challenges, including the high replacement cost of battery electric buses (BEBs) and range anxiety issues (Zhou et al., 2021). In response, governments are progressively promoting BFE by helping transit agencies purchase or lease low- or no- emission vehicles (Federal Transit Administration, 2022). Concurrently, extensive research focuses on charging infrastructure planning and BEB scheduling for solving range anxiety issues (Perumal et al., 2022). In recent years, governments and transit agencies have encountered a new challenge: the sharp expansion of BEB adoption on public transport (PT) without energy power networks' adjustments will counteract the effort of reducing carbon emissions. Current research is increasingly focused on exploring the viability of renewable energy-powered charging infrastructures.

\* Corresponding author.

E-mail address: [xiaolei@buaa.edu.cn](mailto:xiaolei@buaa.edu.cn) (X. Ma).

Among them, solar photovoltaic (PV) energy is a promising solution to enhance the “green” impact of transportation electrification on the environment (Ramadhani et al., 2021; Jirdehi & Tabar, 2023). For example, integrating PV charging infrastructure and electric vehicles represents a sustainable development mode for transportation electrification (Calise et al., 2021). Recent studies have begun to investigate solar-powered electric bus networks for reducing grid dependence and carbon emissions (Ren et al., 2022a; Ren et al., 2022b). However, such solar-powered electric bus networks may lead to discounted performance incurred by the mismatch between PV power production and charging demand. Hence, the solar PV and energy storage system (PESS) is considered to be a feasible solution to the mismatch between power supply and demand mentioned above (Chandra Mouli et al., 2016; Felipe Cortés Borray et al., 2021).

As power battery capacities fade over the years, the mismatch between the actual battery capacities of bus fleets and the working load of the corresponding bus routes has arisen. This mismatch would further aggravate battery capacity fading. Hence, it is crucial to dynamically match the power batteries of bus fleets with appropriate bus depots or bus routes. Therefore, one new and pressing issue is emerging naturally: How should transit agencies determine an optimal plan for power battery replacement and matching by considering battery capacity fading, charging costs, carbon emission costs, and battery replacement costs? With the adoption of BEBs on urban transit system networks, the underlying charging demand for BEBs increases rapidly (Yang et al., 2021). A significant consequence is the need to replace many batteries that have undergone capacity fading (Slattery et al., 2021). When transit agencies deploy PESS at bus charging stations or bus depots, the echelon utilization market for power batteries arises in a closed industrial chain with PT (Lai et al., 2021). Transit agencies purchase new batteries for bus fleets while recycling companies recycle and process retired batteries. The retired batteries are sorted and regrouped by echelon

utilization companies. Transit agencies purchase echelon utilization batteries at a lower price than new batteries. Hence, the second-hand utilization of retired batteries reduces the high purchase cost of new batteries for energy storage systems (ESSs), which is a potential remedy for high demand charges from fast charging (He et al., 2019). A new technical issue emerges when PESS is deployed at bus charging stations. Transit agencies should plan for battery replacement of ESSs by considering the sum of battery replacements, vehicle charging, and carbon emission costs. The battery replacement costs will increase sharply if transit agencies keep a high frequency of battery replacement of ESSs (Zhang et al., 2021). Conversely, the economic benefits of PESS will be reduced if transit agencies keep a low-frequency battery replacement in ESSs. Consequently, models and methods for devising an optimal plan for battery replacement in ESSs need to be proposed.

The capacity fading rates of lithium-ion batteries are highly related to the ranges of discharge and charge cycles (Lam & Bauer, 2013). In general, the higher the working load of the bus fleets, the higher the capacity fading rates of the batteries. The daily working load of the fleet is determined by the fleet size, state of health (SoH) of the batteries, and bus routes (Wang et al., 2020). Thus, matching the power batteries of bus fleets to bus routes or depots at each operational stage (year) is of strategic importance. Besides power battery matching, the battery replacement schedule for each bus in the fleet should naturally be optimized. The prevailing standard for retiring batteries in China is when the actual capacity declines below 80% of the initial capacity (Sathre et al., 2015). However, this widely accepted retirement standard has a notable drawback: BEBs often retain operational viability even after reaching this capacity threshold. This study removes the fixed battery retirement threshold by allowing the buses’ batteries to be replaced at reasonable SoH, thereby extending the life cycles of the batteries.

Currently, experiment results about lithium-ion battery capacity

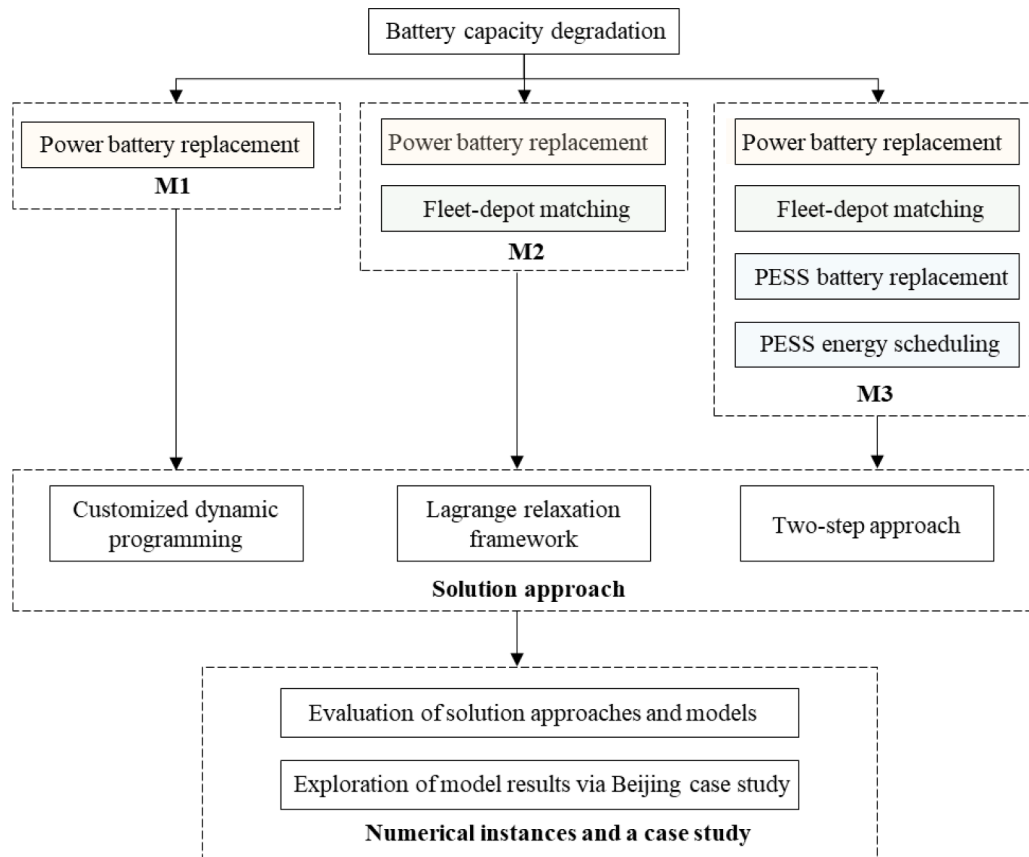


Fig. 1. The overall study framework of this paper.

fading reported in the literature suggest a nonlinear relationship between the capacity fading rate and the depth of discharge (DoD) (Peterson et al., 2010; Bashash et al., 2011; Zhou et al., 2011). Most empirical models for capacity fading rates are highly nonlinear, resulting in intractable optimization models of power battery replacement and matching when commercial solvers are used directly. Similarly, such nonlinear relationships between the capacity fading rate and DoD are applicable to energy storage batteries. Thus, one would fail to solve optimization models associated with battery replacement of ESSs directly via commercial solvers. As the battery capacity degenerates, the BEB scheduling has to be adjusted. For example, the charging times of BEBs must be increased with the decline of their battery capacity. Therefore, the BEB scheduling should be formulated explicitly as an integral part of the optimization models. BEB scheduling and nonlinear empirical models of capacity fading rates will undoubtedly increase the difficulty of modeling and solving these planning and operational challenges.

### 1.2. Objective and contribution

To date, no studies have investigated the power battery replacement and fleet-depot matching problem for a long-term operation stage under the solar-powered electric bus network. To fill this gap, this study proposes a comprehensive framework for sustainable battery scheduling and echelon utilization. The framework considers battery capacity fading and bus charging infrastructure integrated with PESS. We present three mixed integer nonlinear programming models for handling three problems. Model 1 (M1) describes a power battery replacement problem (PBRP) in which the battery replacement plan is optimized while power batteries of bus fleets are not allowed to be matched to other bus routes. Model 2 (M2) models a joint power battery replacement and fleet-depot matching problem (PBRMP) in which PESS is not introduced. The matching problem in some existing literature is also called a bus fleet transition problem. Finally, model 3 (M3) represents the power battery replacement and matching problem by considering PESS (PBRMP-PESS). Comparing M3 with M1 and M2 helps to explore the impacts of introducing PESS on the operating costs and environmental benefits of BEB systems during the entire lifespan.

Our contributions can be summarized as follows. This study represents the first attempt to address the power battery replacement and vehicle-depot matching problem by simultaneously considering PESS. In addition, we incorporate a flow-based BEB scheduling formulation into this framework to establish the explicit relationship between battery capacity fading and BEB scheduling. We present a customized dynamic programming (DP) algorithm to solve the nonlinearity of PBRP. For PBRMP, the solution space is extended to multi-fleet and multi-depot, thereby designing a dual decomposition framework employing Lagrange relaxation (LR) to relax coupling constraints. For PBRMP-PESS, we propose a two-step solution approach. Practical insights from numerical experiments and a case study in Beijing are summarized to help transit agencies establish a sustainable development pathway for bus fleet electrification.

### 1.3. Organization

The rest of this paper is organized as follows. Section 2 reviews the related research. Section 3 formulates three models for PBRP, PBRMP, and PBRMP-PESS. The corresponding solution approaches are presented in Section 4. The computational efficiency of the solution approaches and result comparison of the three models are shown and discussed in Section 5.1 for synthetic instances. Section 5.2 shows the application of the three models to the case study in Beijing, China. The conclusions of this study are drawn, and future research directions are provided in Section 6. Fig. 1 illustrates the overall study framework of this paper.

## 2. Literature review

This study presents a sustainable battery scheduling and echelon utilization framework that integrates battery replacement scheduling and fleet-depot matching by considering battery capacity degradation and PESS. We review the related studies on BEB charging problems by considering battery degradation, bus fleet transition problems, and solar-powered BEB charging infrastructure planning and operating problems.

### 2.1. BEB charging problems by considering battery capacity degradation

The daily working load patterns of BEBs significantly influence the lifespan of on-board lithium batteries. Daily BEB scheduling should consider the impacts of the daily working load patterns on battery capacity degradation. Zhang et al. (2020) investigated the impact of battery capacity degradation on the BEB lifecycle costs. Their simulation results found that the BEB lifespan could be extended by three years, and battery costs could be reduced by 24.7% when optimizing the bus charging schedule by considering battery capacity degradation. Furthermore, Zhang et al. (2021) added battery capacity fading cost into the joint optimization model of BEB scheduling by optimizing charging strategies, and the case study results revealed that the total system cost could be reduced by 10.1%–27.3%. Different working load intensities of BEBs on different routes lead to varying battery fading rates. Wang et al. (2020) proposed a fleet-route matching model for BEBs. The model allocated the BEBs with the lowest battery fading rate to the bus routes with the highest working intensity. However, this model ignored the technical performance differences, such as driving range and charging power, and the impacts of factors such as charging facility layout and bus route characteristics, resulting in low fleet-route matching efficiency. Zang et al. (2022) compared three types of battery fading cost functions: a nonlinear function related to discharge depth, a linear function related to the number of charging and discharging cycles, and a linear function related to the total travel distance. The results showed that the model integrated with nonlinear depreciation functions can reduce the total system cost by 9%–10%.

### 2.2. Bus fleet transition problems

Pelletier et al. (2019) defined the bus fleet transition problem as an integer linear programming model that involved the task assignments for buses, bus purchase, and charger deployment at each period. The optimization model minimized the total cost of bus purchase costs, midlife costs, salvage revenues, operating costs, charging infrastructure construction costs, and demand charges for the entire transition planning horizon. Zhang et al. (2022) focused on the seasonal differences in battery capacity, bus scheduling, charging facility deployment, and bus fleet replacement during the long term. The real-world case study showed that for a bus network consisting of 16 routes, gradually replacing traditional fuel buses with electric buses within eight time periods reduced the total system cost by 17.8% and carbon dioxide emissions by 39.3%.

### 2.3. Solar-powered BEB charging infrastructure planning and operating problems

BFE could place additional strain on the distribution network. To reduce the net charging loads from the grid, Majumder et al. (2019) designed a sustainable electric bus network system by introducing high-capacity batteries and distributed solar PV generation. The experiment results showed that the proposed system framework is feasible in catering to BEB charging demands without additional charging loads to the grid. Liu et al. (2022) proposed a location problem of BEB charging infrastructure integrated with PESS at the bus network level. A two-stage stochastic programming model was established, and the

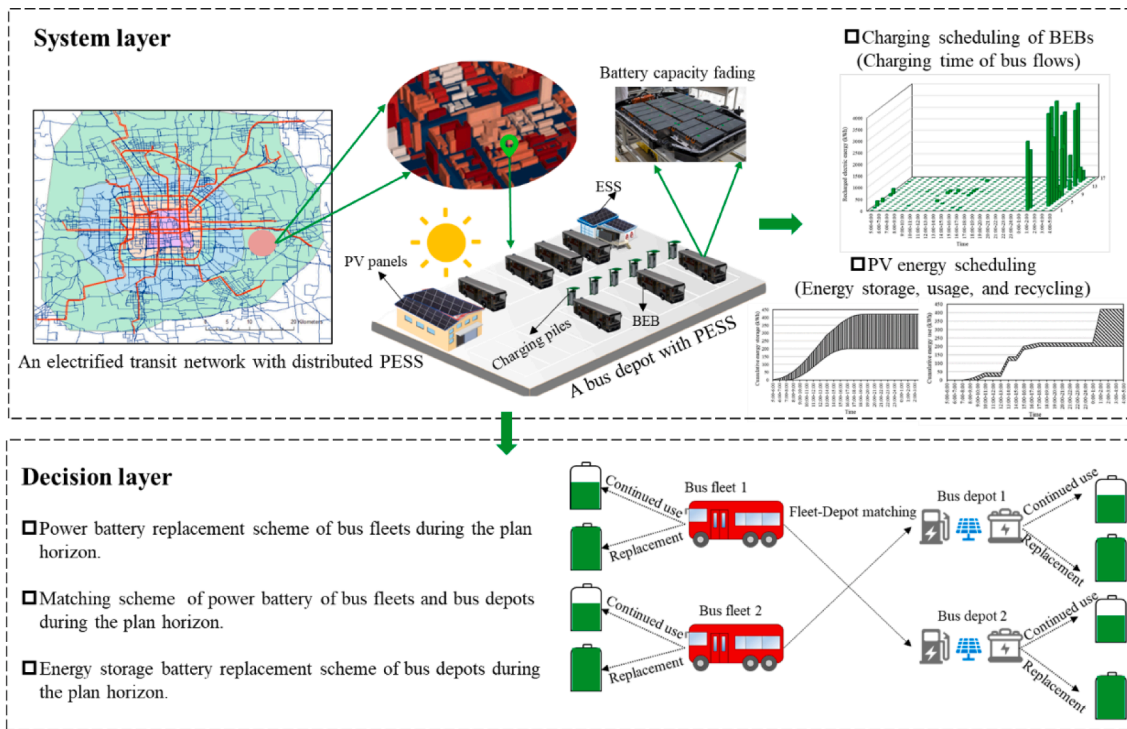


Fig. 2. Illustration of an electric bus network with distributed PESS.

L-shaped algorithm based on sample average approximation was developed to improve the solution efficiency. Liu et al. (2023a) presented a data-driven framework to examine the economic and environmental impacts of implementing PESS within electric bus systems. The optimal PESS configuration was identified by a simulation-based surrogate model-based optimization method. The results of a case study in Beijing revealed that PESS can reduce the system's total cost by 1.5%-6%, charging costs by 11.4%-21.7%, and carbon dioxide emissions by 6.5%-13.3%. Ren et al. (2022a) optimized the deployment of rooftop PV systems to improve clean energy usage for electric buses in high-density cities. A heuristic-based solution approach was designed to solve high-dimensional and nonlinear optimization problems. The case study of 28 bus routes in Hong Kong was explored, and the results indicated that the proposed model could find a cost-effective pathway to deploy PV panels and battery storage systems. Furthermore, Ren et al. (2022b) optimized the BEB charging schedule to improve solar energy on-site consumption, and this BEB charging scheduling problem was formulated as a mixed integer linear programming model. The results of the case study showed that the presented BEB charging strategy can improve the utilization of solar PV energy.

### 3. Model formulation

In this section, we present three models to formulate the PBRP, PBRMP, and PBRMP-PESS, also identified as M1, M2, and M3, respectively. The assumptions used in this study are as follows: (a) Bus charging infrastructures are deployed at bus depots without loss of generality; (b) Fleet sizes are given and fixed; (c) In the carbon trade market, carbon emissions can be traded among companies or entities at official prices. Assumption 3 reveals that the equivalent monetary cost of carbon emissions should be accounted for when transit agencies make decisions. Fig. 2 shows a schematic of an electric bus network with distributed PESS. The illustration of the decisions, which are the focus of this study, is also shown in the Fig. 2.

#### 3.1. Battery capacity degradation

A practical capacity fading or wear model can be combined with other models to design objective functions for optimization models in electric mobility problems (Han et al., 2014). The battery fading depends on three key stress factors (Zhang et al., 2019): SoC (or incremental DoD) (i.e., incremental DoD is the difference between the initial and final SoCs before a cell is recharged to the initial SoC), discharge C-rate, and temperature. This study will not specify the temperature and discharge C-rate as we can assume that the temperature and discharge C-rate are constant while modeling battery fading. We introduce the following equations to calculate the capacity fading rate (Han et al., 2014; Zhang et al., 2021).

$$\xi(SoC_{final}, SoC_{initial}) = \gamma_1 SoC_{dev} e^{\gamma_2 SoC_{avg}} + \gamma_3 e^{\gamma_4 SoC_{dev}}, \quad (1)$$

$$SoC_{avg} = \frac{SoC_{initial} + SoC_{final}}{2}, \quad (2)$$

$$SoC_{dev} = \frac{SoC_{initial} - SoC_{final}}{2}, \quad (3)$$

Where  $\gamma_1, \gamma_2, \gamma_3,$  and  $\gamma_4$  are model parameters.  $\xi(SoC_{final}, SoC_{initial})$  represents the capacity fading rate when the battery is cycled between  $SoC_{initial}$  and  $SoC_{final}$ .  $SoC_{avg}$  denotes the average SoC, and  $SoC_{dev}$  denotes the SoC deviation.

#### 3.2. M1: PBRP

In PBRP, transit agencies determine a one-to-one relationship between bus fleets and depots before the planning horizon. Bus fleets are not allowed to be reallocated to bus depots during the entire planning horizon. M1 describes a power battery replacement problem in bus fleets. Variables and constraints of multi-fleet and multi-depot do not exist in M1. Hence, for each specific bus fleet  $f$ , M1 is presented as follows:

$$\min \alpha_1 \sum_{\varphi} N_f z_{f\varphi}^b - \alpha_2 \sum_{\varphi} N_f E_{f\varphi-1} z_{f\varphi}^b + \sum_{\varphi} \sum_m D_m \sum_t (\delta_{gr} + \lambda_t) g_{f\varphi}, \quad (4)$$

$$E_{f\varphi}^i = E_{f\varphi-1}^i (1 - z_{f\varphi}^b) + \bar{E}_f z_{f\varphi}^b, \forall \varphi \in \Gamma, \quad (5)$$

$$E_{f\varphi} = E_{f\varphi}^i - \xi_{f\varphi}^b, \forall \varphi \in \Gamma, \quad (6)$$

$$h_{f\varphi}^i + h_{f\varphi} + \sum_{r \in R_f} \bar{y}_{r,t} = N_f, \forall t \in T, \varphi \in \Gamma, \quad (7)$$

$$h_{f\varphi} \leq c_w \cdot 1, \forall t \in T, \varphi \in \Gamma, \quad (8)$$

$$g_{f\varphi} = p_{gr} h_{f\varphi}, \forall t \in T, \varphi \in \Gamma, \quad (9)$$

$$\eta_{\min} E_{f\varphi}^i N_f \leq E_{f\varphi}^i N_f - \sum_{i \leq t} \sum_{r \in R_f} \bar{y}_{r,t} e_r + \sum_{i \leq t} g_{f\varphi}, \quad (10)$$

$$\forall t \in T, \varphi \in \Gamma,$$

$$E_{f\varphi}^i N_f \geq E_{f\varphi}^i N_f - \sum_{i \leq t} \sum_{r \in R_f} \bar{y}_{r,t} e_r + \sum_{i \leq t} g_{f\varphi}, \quad (11)$$

$$\forall t \in T, \varphi \in \Gamma,$$

$$\sum_{t \in T} g_{f\varphi} - \sum_{i \in T} \sum_{r \in R_f} \bar{y}_{r,t} e_r = 0, \forall \varphi \in \Gamma, \quad (12)$$

$$z_{f\varphi}^b \in \{0, 1\}, \forall \varphi \in \Gamma, \quad (13)$$

$$E_{f\varphi}^i \geq 0, \forall \varphi \in \Gamma, \quad (14)$$

$$E_{f\varphi} \geq 0, \forall \varphi \in \Gamma, \quad (15)$$

$$h_{f\varphi}^i \geq 0, \forall t \in T, \varphi \in \Gamma, \quad (16)$$

$$h_{f\varphi} \geq 0, \forall t \in T, \varphi \in \Gamma, \quad (17)$$

$$g_{f\varphi} \geq 0, \forall t \in T, \varphi \in \Gamma. \quad (18)$$

Let  $\alpha_1$  denote the price of purchasing a power battery with a certain capacity. Let  $\alpha_2$  denote the recycling price of 1 kWh of retired power batteries. Let  $N_f$  denote the size of bus fleet  $f$ . Let  $D_m$  denote the number of days in month  $m$ . We use  $\delta_{gr}$  to denote the carbon emission cost of 1 kWh of electricity produced by coal-fired power plants. Let  $\lambda_t$  indicate the electricity price at hour  $t$ . Let  $z_{f\varphi}^b$  denote a binary variable where it is set to 1 if the transit agency purchases new batteries for bus fleet  $f$  at the beginning of year  $\varphi$ , and set to 0 otherwise. The continuous variable  $E_{f\varphi}^i$  denote the current capacity of batteries associated with bus fleet  $f$  at the end of year  $\varphi$ . Let the continuous variable  $g_{f\varphi}$  denote the total recharged electric energy of bus fleet  $f$  at hour  $t$  and year  $\varphi$ . Objective function (4) minimizes the sum of battery replacement, charging, and carbon emission costs.

Constraint (5) determines the relationship between  $E_{f\varphi}^i$  and  $E_{f\varphi-1}$ , where let  $E_{f\varphi}^i$  denote the current capacity of batteries associated with bus fleet  $f$  after the decision of battery replacement is made at the beginning of year  $\varphi$ . Constraint (6) defines the relationship between  $E_{f\varphi}^i$  and  $E_{f\varphi}$ .

Let  $\bar{y}_{r,t}$  denote the number of service trips at hour  $t$  for bus route  $r$ . Let  $t_r$  denote the travel time of a round-trip for bus route  $r$ . The continuous variable  $h_{f\varphi}^i$  represents the total layover time of bus fleet  $f$  at hour  $t$  and year  $\varphi$ . The continuous variable  $h_{f\varphi}$  indicates that the total recharging time of bus fleet  $f$  at hour  $t$  and year  $\varphi$ . Constraint (7) establishes an explicit relationship between bus flow and fleet size via the time conservation principle. Constraint (8) ensures that the total charging time of bus fleet  $f$  at hour  $t$  and year  $\varphi$  is less than the supply  $c_w \cdot 1$ , where  $c_w$  is the number of chargers installed at the bus depot  $w$  associated with bus fleet  $f$ . Constraint (9) defines the total recharged electric energy for bus fleet

at hour  $t$  and year  $\varphi$ , where  $p_{gr}$  represents the charging power of chargers.

Let  $\eta_{\min}$  denote the allowable minimum SoC. Let  $e_r$  denote the energy consumption of an electric bus driving along route  $r$ . Constraint (10) ensures that the current total electric energy of bus fleet  $f$  at hour  $t$  and year  $\varphi$  should be greater than or equal to  $\eta_{\min} E_{f\varphi}^i N_f$ . Constraint (11) ensures that the current total electric energy of bus fleet  $f$  at hour  $t$  and year  $\varphi$  should be less than or equal to  $E_{f\varphi}^i N_f$ . Constraint (12) imposes that bus fleet  $f$  should be fully charged at the end of a day. Constraints (13)–(18) define the types and ranges of the decision variables.

According to objective function (1), the amount of reduced battery capacity of a bus fleet depends on BEB scheduling. In this study, BEB scheduling is modeled via a flow-based formulation to lighten the computational burden. Without specific schedules of BEBs, we present the following rules to estimate  $\xi_{f\varphi}^b$ :

**Case 1:** For  $\frac{\sum_t g_{f\varphi}}{E_{f\varphi}^i N_f} \leq 1 - \eta_{\min}$ , let  $SoC_{final} = 1 - \frac{\sum_t g_{f\varphi}}{E_{f\varphi}^i N_f}$  and  $SoC_{initial} = 1$ .

$\xi_{f\varphi}^b$  can be obtained as follows:

$$\xi_{f\varphi}^b = 365 \times (\gamma_1 SoC_{dev} e^{\gamma_2 SoC_{avg}} + \gamma_3 e^{\gamma_4 SoC_{dev}}) \times 2 \times E_{f\varphi}^i \times \frac{\sum_t g_{f\varphi}}{E_{f\varphi}^i N_f}, \quad (19)$$

where  $\sum_t g_{f\varphi}$  represents the total charging demand of bus fleet  $f$  in a day.

Let  $E_{f\varphi}^i N_f$  be the total energy supply of bus fleet  $f$  without recharging

during the service period. Thus,  $\frac{\sum_t g_{f\varphi}}{E_{f\varphi}^i N_f}$  represents the average battery

usage rate of bus fleet  $f$ . If  $\frac{\sum_t g_{f\varphi}}{E_{f\varphi}^i N_f} \leq 1 - \eta_{\min}$ , then the final SoC of a BEB in

bus fleet  $f$  will equal  $1 - \frac{\sum_t g_{f\varphi}}{E_{f\varphi}^i N_f}$ . In equation (19),  $2 \times E_{f\varphi}^i \times \frac{\sum_t g_{f\varphi}}{E_{f\varphi}^i N_f}$  represents the average amount of cycled energy of a battery.

**Case 2:** For  $\frac{\sum_t g_{f\varphi}}{E_{f\varphi}^i N_f} > 1 - \eta_{\min}$ , let  $q^* = \min\{q \mid \frac{\sum_t g_{f\varphi}}{q E_{f\varphi}^i N_f} \leq 1 - \eta_{\min}, q \in Z^+\}$ ,

$SoC_{final} = 1 - \frac{\sum_t g_{f\varphi}}{q^* E_{f\varphi}^i N_f}$  and  $SoC_{initial} = 1$ . We can obtain  $\xi_{f\varphi}^b$  as follows:

$$\xi_{f\varphi}^b = q^* \cdot 365 \cdot (\gamma_1 SoC_{dev} e^{\gamma_2 SoC_{avg}} + \gamma_3 e^{\gamma_4 SoC_{dev}}) \cdot 2 \cdot E_{f\varphi}^i \cdot \frac{\sum_t g_{f\varphi}}{q^* E_{f\varphi}^i N_f}, \quad (20)$$

where  $\frac{\sum_t g_{f\varphi}}{q^* E_{f\varphi}^i N_f}$  represents the average battery usage rate of bus fleet  $f$ . Let

$2 \cdot E_{f\varphi}^i \cdot \frac{\sum_t g_{f\varphi}}{q^* E_{f\varphi}^i N_f}$  represent the average cycled energy of a battery.

### 3.3. M2: PBRMP

In PBRMP, power batteries of bus fleets are allowed to be reallocated to bus depots during the planning horizon. Consequently, variables and constraints of multi-fleet and multi-depot arise in M2, leading to the following formulation:

$$\min \alpha_1 \sum_{\varphi} \sum_f N_f z_{f\varphi}^b - \alpha_2 \sum_{\varphi} \sum_f N_f E_{f\varphi-1} z_{f\varphi}^b + \sum_{\varphi} \sum_m D_m \sum_f \sum_t (\delta_{gr} + \lambda_t) g_{f\varphi}, \quad (21)$$

$$\sum_{w \in W} x_{fw\varphi} = 1, \forall f \in F, \varphi \in \Gamma, \quad (22)$$

$$\sum_{f \in F} x_{fw\varphi} = 1, \forall w \in W, \varphi \in \Gamma, \quad (23)$$

$$E_{f\varphi}^i = E_{f\varphi-1}^i (1 - z_{f\varphi}^b) + \bar{E}_f z_{f\varphi}^b, \forall f \in F, \varphi \in \Gamma, \quad (24)$$

$$E_{f\varphi} = E'_{f\varphi} - \xi_{f\varphi}^b, \forall f \in F, \varphi \in \Gamma, \quad (25)$$

$$h'_{ft\varphi} + h_{ft\varphi} + \sum_{w \in W} \left( \sum_{r \in R_w} \bar{y}_{r,t} \right) x_{f\varphi w} = N_f, \forall f \in F, t \in T, \varphi \in \Gamma, \quad (26)$$

$$h_{ft\varphi} \leq \left( \sum_{w \in W} c_w x_{f\varphi w} \right) \cdot 1, \forall f \in F, t \in T, \varphi \in \Gamma, \quad (27)$$

$$g_{ft\varphi} = p_{gr} h_{ft\varphi}, \forall f \in F, t \in T, \varphi \in \Gamma, \quad (28)$$

$$\eta_{\min} E'_{f\varphi} N_f \leq E'_{f\varphi} N_f - \sum_{i \leq t} \sum_{w \in W} \left( \sum_{r \in R_w} \bar{y}_{r,i} e_r \right) x_{f\varphi w} + \sum_{i \leq t} g_{fi\varphi}, \forall f \in F, t \in T, \varphi \in \Gamma, \quad (29)$$

$$E'_{f\varphi} N_f \geq E'_{f\varphi} N_f - \sum_{i \leq t} \sum_{w \in W} \left( \sum_{r \in R_w} \bar{y}_{r,i} e_r \right) x_{f\varphi w} + \sum_{i \leq t} g_{fi\varphi}, \forall f \in F, t \in T, \varphi \in \Gamma, \quad (30)$$

$$\sum_{i \in T} g_{fi\varphi} - \sum_{i \in T} \sum_{w \in W} \left( \sum_{r \in R_w} \bar{y}_{r,i} e_r \right) x_{f\varphi w} = 0, \forall f \in F, \varphi \in \Gamma, \quad (31)$$

$$x_{f\varphi w} \in \{0, 1\}, \forall f \in F, w \in W, \varphi \in \Gamma, \quad (32)$$

$$z_{f\varphi}^b \in \{0, 1\}, \forall f \in F, \varphi \in \Gamma, \quad (33)$$

$$E'_{f\varphi} \geq 0, \forall f \in F, \varphi \in \Gamma, \quad (34)$$

$$E'_{f\varphi} \geq 0, \forall f \in F, \varphi \in \Gamma, \quad (35)$$

$$h'_{ft\varphi} \geq 0, \forall f \in F, t \in T, \varphi \in \Gamma, \quad (36)$$

$$h_{ft\varphi} \geq 0, \forall f \in F, t \in T, \varphi \in \Gamma, \quad (37)$$

$$g_{ft\varphi} \geq 0, \forall f \in F, t \in T, \varphi \in \Gamma. \quad (38)$$

Objective function (21) minimizes the sum of power battery replacement, charging, and carbon emission costs. Let  $x_{f\varphi w}$  denote a binary variable in which it is set to 1 if power batteries of bus fleet  $f$  are reallocated to bus depot  $w$  at the beginning of year  $\varphi$ , and set to 0 otherwise. Constraints (22) and (23) jointly ensure the one-to-one relationship between bus fleets and bus routes. Other parameters, variables, and constraints in M2 have been inherited from M1.

### 3.4. M3: PBRMP-PESS

M3 formulates PBRMP-PESS in which the battery matching, battery replacement for BEBs, and battery replacement for ESSs are jointly optimized when transit agencies deploy PESS at bus depots. M3 inherits constraints (22)–(38) of M2 and develops a new objective function and constraints as follows:

$$\begin{aligned} \min \alpha_1 & \sum_{\varphi} \sum_f N_f z_{f\varphi}^b - \alpha_2 \sum_{\varphi} \sum_f N_f E'_{f\varphi} - 1 z_{f\varphi}^b \\ & + \alpha_3 \sum_{\varphi} \sum_w \bar{C}_w z_{w\varphi}^s - \alpha_4 \sum_{\varphi} \sum_w C_{w\varphi-1} z_{w\varphi}^s \\ & + \sum_{\varphi} \sum_m D_m \sum_w \sum_t [(\delta_{pv} - \delta_{gr} - \lambda_t) u_{mtw\varphi} - \lambda'_t (o_{\varphi} A_w P_{mt} - v_{mtw\varphi})] \\ & + \sum_{\varphi} \sum_m D_m \sum_f \sum_t (\delta_{gr} + \lambda_t) g_{ft\varphi} \end{aligned} \quad (39)$$

$$C'_{w\varphi} = C_{w\varphi-1} (1 - z_{w\varphi}^s) + \bar{C}_w z_{w\varphi}^s, \forall w \in W, \varphi \in \Gamma, \quad (40)$$

$$C_{w\varphi} = C'_{w\varphi} - \xi_{w\varphi}^s, \forall w \in W, \varphi \in \Gamma, \quad (41)$$

$$v_{mtw\varphi} \leq o_{\varphi} A_w P_{mt}, \forall w \in W, t \in T, m \in M, \varphi \in \Gamma, \quad (42)$$

$$u_{mtw\varphi} - \sum_{f \in F} g_{ft\varphi} x_{f\varphi w} \leq 0, \forall w \in W, t \in T, m \in M, \varphi \in \Gamma, \quad (43)$$

$$\sum_{s=1}^t (v_{mtw\varphi} - u_{mtw\varphi}) \leq C'_{w\varphi}, \forall w \in W, t \in T, m \in M, \varphi \in \Gamma, \quad (44)$$

$$\sum_{s=1}^t (v_{mtw\varphi} - u_{mtw\varphi}) \geq 0, \forall w \in W, t \in T, m \in M, \varphi \in \Gamma, \quad (45)$$

$$C'_{w\varphi} \geq 0, \forall w \in W, \varphi \in \Gamma, \quad (46)$$

$$C_{w\varphi} \geq 0, \forall w \in W, \varphi \in \Gamma, \quad (47)$$

$$u_{mtw\varphi} \geq 0, \forall w \in W, t \in T, m \in M, \varphi \in \Gamma, \quad (48)$$

$$v_{mtw\varphi} \geq 0, \forall w \in W, t \in T, m \in M, \varphi \in \Gamma, \quad (49)$$

$$z_{w\varphi}^s \in \{0, 1\}, \forall w \in W, \varphi \in \Gamma. \quad (50)$$

Let  $\alpha_3$  denote the price of 1 kWh of echelon utilization batteries. Let  $\alpha_4$  denote the recycling price of 1 kWh of echelon utilization batteries. We use  $\bar{C}_w$  to denote the initial capacity of the energy storage system at bus depot  $w$ .  $\delta_{pv}$  represents the carbon emission cost of 1 kWh of electricity produced via PV power generation. Let  $\lambda'_t$  denote the price of PV electricity energy recycling at hour  $t$ . Let  $o_{\varphi}$  denote the power fading rate of PV modules at year  $\varphi$ . We use  $A_w$  to denote the number of PV modules installed at bus depot  $w$ . Let  $p_{mt}$  denote the power output of the PV module at hour  $t$  and month  $m$ . We use  $z_{w\varphi}^s$  to denote a binary variable where it is set to 1 if the transit agency purchases echelon utilization batteries for energy storage of bus depot  $w$  at the beginning of year  $\varphi$ , and set to 0 otherwise. The continuous variable  $C_{w\varphi}$  denote the current total capacity of energy storage of bus depot  $w$  at the end of year  $\varphi$ . The continuous variable  $u_{mtw\varphi}$  indicates that the amount of PV electricity released from energy storage for charging at bus depot  $w$  at hour  $t$  in month  $m$  of year  $\varphi$ . The continuous variable  $v_{mtw\varphi}$  represents the amount of PV electricity flowing into energy storage for charging at bus depot  $w$  at hour  $t$  in month  $m$  of year  $\varphi$ . Objective function (39) minimizes the sum of battery replacement for BEBs and ESSs, charging, and carbon emission costs.

Constraint (40) determines the relationship between  $C'_{w\varphi}$  and  $C_{w\varphi-1}$ , where the continuous variable  $C'_{w\varphi}$  represents the current total capacity of energy storage of bus depot  $w$  after the decision of battery replacement is made at the beginning of year  $\varphi$ . Constraint (41) defines the relationship between  $C'_{w\varphi}$  and  $C_{w\varphi}$ .

Constraint (42) ensures that the amount of PV electricity flowing into the ESS is less than or equal that of PV power generation at bus depot  $w$ . Constraint (43) ensures that the amount of PV electricity released from the ESS for charging is less than or equal to the charging demand at bus depot  $w$ . Constraints (44) and (45) jointly define the range of the current storage at bus depot  $w$  at hour  $t$  in month  $j$  of year  $\varphi$ . Constraints (46)–(50) define the types and ranges of decision variables.

## 4. Solution approach

### 4.1. DP reformulation for M1

Commercial solvers are inefficient in solving M1 directly due to the nonlinear capacity fading model employed in this study. Solvers designed for nonlinear programming often struggle to guarantee optimal solutions for problems with complex nonlinear structures like our models. To obtain an exact solution, we reformulate M1 as a DP, a variant of classic equipment replacement problems (Sullivan et al., 2002). The basic elements of DP in M1 are presented as follows.

The stage of the DP model is denoted by year  $\varphi$ . The decision of DP is  $z_{f\varphi}^b$  and the state of each stage in DP is denoted by  $E_{f\varphi}$ . The following proposition is used to determine  $h'_{f\varphi}$ ,  $h_{f\varphi}$ , and  $g_{f\varphi}$ .

**Proposition 1.** *The solution of  $h'_{f\varphi}$ ,  $h_{f\varphi}$ , and  $g_{f\varphi}$  at stage  $\varphi$  can be obtained by solving the following linear programming when  $z_{f\varphi}^b$  is given.*

$$\min \sum_m D_m \sum_t (\delta_{gr} + \lambda_t) g_{f\varphi}, \quad (51)$$

$$h'_{f\varphi} + h_{f\varphi} + \sum_{r \in R_f} \bar{y}_{r,t} = N_f, \forall t \in T, \quad (52)$$

$$h_{f\varphi} \leq c_f \cdot 1, \forall t \in T, \quad (53)$$

$$g_{f\varphi} = p_{gr} h_{f\varphi}, \forall t \in T, \quad (54)$$

$$\eta_{\min} E'_{f\varphi} N_f \leq E'_{f\varphi} N_f - \sum_{i \leq t} \sum_{r \in R_f} \bar{y}_{ri} e_r + \sum_{i \leq t} g_{fi\varphi}, \quad (55)$$

$$\forall t \in T,$$

$$E_{f\varphi} N_f \geq E'_{f\varphi} N_f - \sum_{i \leq t} \sum_{r \in R_f} \bar{y}_{ri} e_r + \sum_{i \leq t} g_{fi\varphi}, \forall t \in T, \quad (56)$$

$$\sum_{t \in T} g_{f\varphi} - \sum_{t \in T} \sum_{r \in R_f} \bar{y}_{ri} e_r = 0, \quad (57)$$

$$h'_{f\varphi} \geq 0, t \in T, \quad (58)$$

$$h_{f\varphi} \geq 0, \forall t \in T, \quad (59)$$

$$g_{f\varphi} \geq 0, \forall t \in T. \quad (60)$$

**Proof.** According to equations (29) and (30),  $z_{f\varphi}^b$  is determined by  $E'_{f\varphi}$  and  $\sum_t g_{f\varphi}$ . In addition,  $\sum_t g_{f\varphi}$  is fixed and equals  $\sum_{t \in T} \sum_{r \in R_f} \bar{y}_{ri} e_r$  according to constraint (12). When  $z_{f\varphi}^b$  is given at stage  $\varphi$ ,  $E'_{f\varphi}$  can be obtained according to constraint (5). Hence, the state  $E_{f\varphi}$  is only influenced by  $\sum_t g_{f\varphi}$ . As  $\sum_t g_{f\varphi}$  is fixed, we naturally minimize objective (51) at stage  $\varphi$  to obtain a candidate solution to DP.

**Proposition 1.** means that the decision set of DP is only constituted by  $z_{f\varphi}^b$ . Therefore,  $h'_{f\varphi}$ ,  $h_{f\varphi}$ , and  $g_{f\varphi}$  are recourse variables on  $z_{f\varphi}^b$ . Then, we analyze the computational complexity of the proposed DP.

**Proposition 2.** The linear programming in proposition 1 will be solved at most  $|\Gamma|$  times in DP with a stage set  $\Gamma$ .

**Proof.** Suppose the case that the bus fleet can fulfill all service trips without replacement power batteries during the entire planning horizon. At stage  $\varphi$ , the linear programming in proposition 1 varies with  $E'_{f\varphi}$  because other parameters in linear programming are fixed. There are up to  $\varphi$  different values for  $E'_{f\varphi}$ ,  $\forall \varphi' \leq \varphi$  at the beginning of year  $\varphi$ . The maximum value of  $E'_{f\varphi}$  is  $\bar{E}_f$  when  $z_{f\varphi}^b = 1, \forall \varphi' \leq \varphi$ . The minimum value is

$\bar{E}_f - \sum_1^{\varphi-1} \xi_{f\varphi}^b$  when transit agencies do not replace new batteries for bus fleets for years from 1 to  $\varphi$ . Hence, we know that there are up to  $|\Gamma|$  different values for  $E'_{f\varphi}$ ,  $\forall \varphi' \leq \varphi$  at the beginning of year  $|\Gamma|$ . Consequently, the linear programming in proposition 1 will be solved at most  $|\Gamma|$  times for the DP with a stage set  $\Gamma$ .

### 4.2. LR for M2

Power batteries of bus fleets are allowed to be reallocated among bus depots throughout the entire planning period in M2. The ‘‘curse of dimensionality’’ has to be faced when we use DP to solve M2 directly because variables and constraints of multi-fleet and multi-depot arise in M2 (Powell, 2010). A dual decomposition framework that employs LR to relax coupled constraints is presented to relieve heavy computational burdens.

#### 4.2.1. LR framework

LR is a dual decomposition method in which the coupling constraint (23) in M2 is relaxed and the corresponding Lagrange multiplier  $\pi_{w,\varphi}$  is optimized to find the optimal solution. The LR framework is presented as follows:

##### LR framework for M2

---

Step 1: Initialization  
 Initializing iteration number  $k = 0$ ;  
 Initializing Lagrange multiplier  $\pi_{w,\varphi}$ ;  
 Setting lower bound  $LB^* = -\infty$  and upper bound  $UB^* = +\infty$ .  
 Step 2: Generating the lower bound solution and updating  $LB^*$   
 Step2.1: Generating the lower bound solution by solving sub-problems for each bus fleet  $f$   
 Finding the least-cost solution for bus fleet  $f$  by calling DP.end for  
 Step2.2: Updating  $LB^*$   
 Computing  $LB^k$  using the current solutions to sub-problems;  
 $LB^* = \max\{LB^*, LB^k\}$ .  
 Step 3: Generating the feasible solution and update  $UB^*$   
 Step3.1: Generating the feasible solution by calling Algorithm 1 (explained below);  
 Step3.2: Updating  $UB^*$   
 Step 4: Termination condition  
 Computing the relative gap between  $LB^*$  and  $UB^*$ ;  
 If the current gap is smaller than  $\varepsilon$ , the solution procedure will be terminated.  
 Otherwise, updating the Lagrange multiplier  $\pi_{w,\varphi}$  and returning to step 2. The Lagrange multiplier  $\pi_{w,\varphi}$  is updated as follows:

$$\pi_{w,\varphi} = \pi_{w,\varphi} + \frac{UB^* - LB^*}{\left\| \sum_{f \in F} x_{fw\varphi} - 1 \right\|_2} \left( \sum_{f \in F} x_{fw\varphi} - 1 \right)$$

The relative gap between  $LB^*$  and  $UB^*$  is defined by  $\frac{UB^* - LB^*}{UB^*}$ . The LR framework explicitly provides upper and lower bounds of M2, and a tradeoff can be implemented between solution time and solution accuracy by observing the relative gap. The following algorithm is designed to obtain the feasible solution from the least-cost paths of bus fleets at iteration  $k$ :

---

#### Algorithm 1

---

Step 1: Initialization  
 Setting tabu list  $TL = \emptyset$  and solution list  $SL = \emptyset$ ;  
 Giving the Lagrange multiplier  $\pi_{w,\varphi}$ .  
 Step 2: Generating the feasible solution and updating the tabu list  $TL$  for each bus fleet  $f$   
 Step 2.1: Generating the feasible solution  
 Finding the least-cost solution for bus fleet  $f$  by calling DP and responding to tabu list  $TL$ .  $x_{w,\varphi}$  will be not allowed to be one if tuple  $(w,\varphi)$  is in tabu list  $TL$ .  
 Step 2.2: Updating solution list  $SL$   
 Adding the least-cost solution of bus fleet  $f$  into solution list  $SL$ .  
 Step 2.3: Updating tabu list  $TL$   
 If  $x_{w,\varphi} = 1$ , tuple  $(w,\varphi)$  is added into tabu list  $TL$ .  
 end for

---

#### 4.2.2. Sub-problem

In M2, the coupled constraint (23) across different bus fleets is a single set of hard constraints. With LR, constraint (23) is dualized into

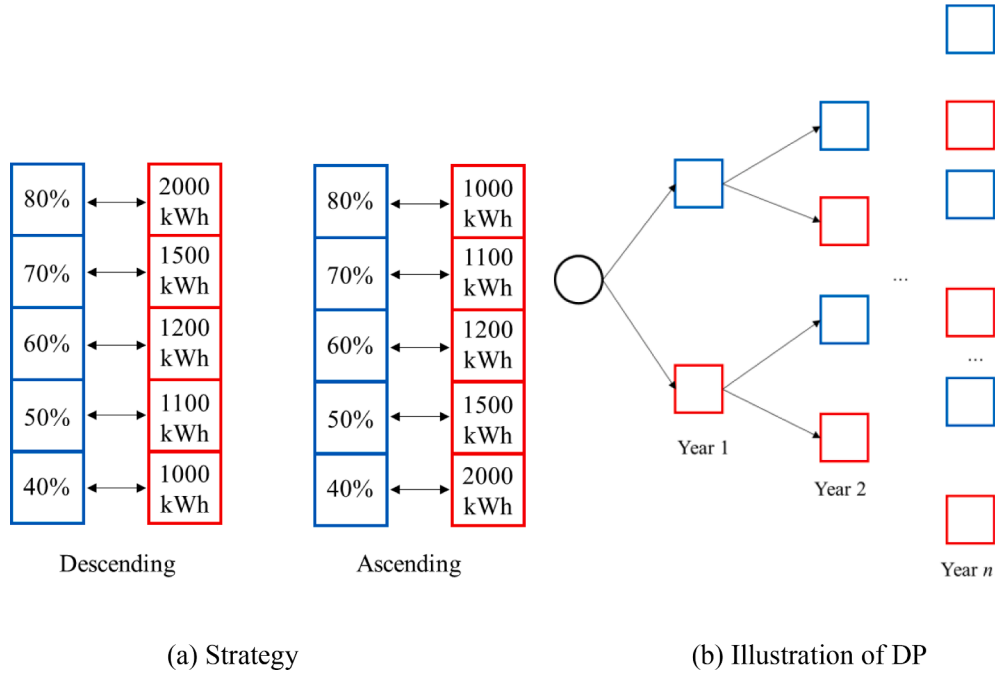


Fig. 3. Illustration of strategy-based DP.

the objective function (21) as (61).

$$\begin{aligned} \min L = & \alpha_1 \sum_{\varphi} \sum_f N_f z_{f\varphi}^b - \alpha_2 \sum_{\varphi} \sum_f N_f E_{f\varphi-1} z_{f\varphi}^b \\ & + \sum_{\varphi} \sum_m D_m \sum_f \sum_t (\delta_{gr} + \lambda_t) g_{ft\varphi} \\ & + \sum_w \sum_{\varphi} \pi_{w\varphi} \left( \sum_{f \in F} x_{f\varphi} - 1 \right), \end{aligned} \quad (61)$$

where  $\pi_{w\varphi}$  is the Lagrange multiplier associated with constraint (23). Naturally, the objective function (61) can be decomposed into sub-problems for each bus fleet  $f$  as follows:

$$\begin{aligned} \min L_f = & \alpha_1 \sum_{\varphi} N_f z_{f\varphi}^b - \alpha_2 \sum_{\varphi} N_f E_{f\varphi-1} z_{f\varphi}^b \\ & + \sum_{\varphi} \sum_m D_m \sum_t (\delta_{gr} + \lambda_t) g_{ft\varphi} \\ & + \sum_w \sum_{\varphi} \pi_{w\varphi} x_{f\varphi} \end{aligned} \quad (62)$$

The lower bound of M2 is further obtained as  $\sum_{f \in L} \min L_f - \sum_w \sum_{\varphi} \pi_{w\varphi}$ .

#### 4.2.3. Customized DP for sub-problems

Objective function (62) involves a mixed integer nonlinear programming because a nonlinear capacity fading model is employed. We can reformulate a DP in which the *stage* of DP is denoted by year  $\varphi$ , the *state* of each stage in DP is denoted by  $E_{f\varphi}$ , and the *decisions* of DP are  $z_{f\varphi}^b$  and  $x_{f\varphi}$ . We can expand proposition 1 for this DP in a straightforward manner. That is the solution of  $h'_{f\varphi}$ ,  $h_{f\varphi}$ , and  $g_{f\varphi}$  at stage  $\varphi$  can be obtained by minimizing objective (51) with constraint (53) and the following constraints when  $z_{f\varphi}^b$  and  $x_{f\varphi}$  are given as follows:

$$h'_{f\varphi} + h_{f\varphi} + \sum_{w \in W} \left( \sum_{r \in R_w} \bar{y}_{rt} e_r \right) x_{f\varphi} = N_f, \forall t \in T, \quad (63)$$

$$h_{f\varphi} \leq \left( \sum_{w \in W} c_w x_{f\varphi} \right) \cdot 1, \forall t \in T, \quad (64)$$

$$\begin{aligned} \eta_{\min} E'_{f\varphi} N_f \leq & E'_{f\varphi} N_f - \sum_{t \leq \varphi} \sum_{w \in W} \left( \sum_{r \in R_w} \bar{y}_{rt} e_r \right) x_{f\varphi} \\ & + \sum_{t \leq \varphi} g_{ft\varphi}, \forall t \in T, \end{aligned} \quad (65)$$

$$\begin{aligned} E'_{f\varphi} N_f \geq & E'_{f\varphi} N_f - \sum_{t \leq \varphi} \sum_{w \in W} \left( \sum_{r \in R_w} \bar{y}_{rt} e_r \right) x_{f\varphi} \\ & + \sum_{t \leq \varphi} g_{ft\varphi}, \forall t \in T, \end{aligned} \quad (66)$$

$$\sum_{t \in T} g_{ft\varphi} - \sum_{t \in T} \sum_{w \in W} \left( \sum_{r \in R_w} \bar{y}_{rt} e_r \right) x_{f\varphi} = 0. \quad (67)$$

The state space of DP in M2 is much larger than that in M1 because the power batteries of bus fleets are allowed to be reallocated to bus depots during the planning period. A heavy burden in computation arises in LR due to the low solution efficiency of DP. Let  $n_1$  and  $n_2$  be two nodes at stage  $\varphi$  of DP. Let  $E_{n_1}$  and  $E_{n_2}$  be the current capacities of BEBs at the end of year  $\varphi$  for  $n_1$  and  $n_2$ , respectively. Let  $C_1$  and  $C_2$  denote the current accumulated costs associated with objective function (62) for  $n_1$  and  $n_2$ , respectively. We present the following proposition to improve the solution efficiency of DP.

**Proposition 3.** At stage  $\varphi$  of DP, there are two nodes  $n_1$  and  $n_2$  with labels  $(E_{n_1}, C_1)$  and  $(E_{n_2}, C_2)$ , respectively. If  $E_{n_1} \geq E_{n_2}$  and  $C_{n_1} \leq C_{n_2}$ , then node  $n_1$  will dominate node  $n_2$ .

**Proof.** We have known that the state  $E_{f\varphi}$  is only influenced by  $\sum g_{ft\varphi}$ . If  $E_{n_1} \geq E_{n_2}$  for nodes  $n_1$  and  $n_2$ , then any feasible solution strategy of years from  $\varphi + 1$  to  $|\Gamma|$  for node  $n_2$  will also be feasible for node  $n_1$ . We assume that there exists an optimal solution  $S^*$ , which includes node  $n_2$  at stage  $\varphi$ . We construct another solution  $S'$  which the solution in years from  $\varphi + 1$  to  $|\Gamma|$  is the same as the optimal solution  $S^*$ . Hence,  $E_{f\varphi}, \varphi' > \varphi$  of  $S'$  is always greater than or equal to  $E_{f\varphi}, \varphi' > \varphi$  of  $S^*$ . Observing constraint (65), we know that objective (51) with the years from  $\varphi + 1$  to  $|\Gamma|$  for  $S'$  is always less than or equal to that for  $S^*$ . Observing objective (62), –

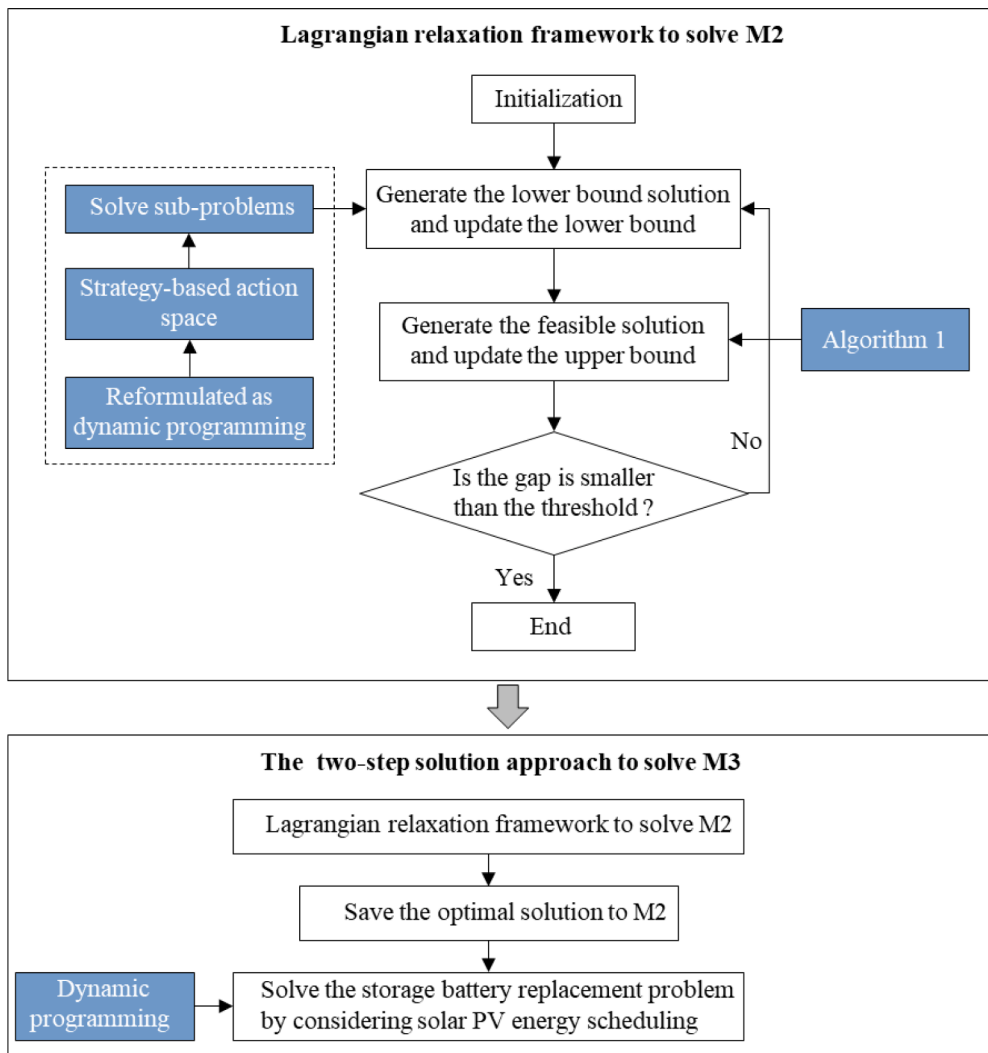


Fig. 4. A flowchart of the solution approaches for M2 and M3.

$\alpha_2 \sum_{\varphi \geq \varphi+1} N_f E_{f\varphi-1} z_{f\varphi}^b$  for  $S'$  is always less than or equal to that for  $S^*$ . Considering that  $C_{n1} \leq C_{n2}$ , the total cost of  $S'$  is less than or equal to that of  $S^*$ . Thus, a contradiction is obtained.

**Proposition 3.** prunes the nodes that are dominated by other nodes at each stage of DP. Besides, a state discretization strategy is employed to reduce the state space of DP. We discretize continuous state  $E_{f\varphi}$  by identical intervals of 2 kWh. Therefore, there are at most  $\lceil \frac{E_f}{2} \rceil$  states for bus fleet  $k$ .

#### 4.3. Two-step solution approach to M3

The LR framework presents a poor performance in M3 due to the slow convergence rate and additional computational burden of solving (39)–(50). The two-step solution approach can obtain a near-optimal solution to M3. In the first step, we solve M2 by using LR and obtain  $z_{f\varphi}^b$ ,  $x_{f\varphi}$ , and  $g_{f\varphi}$ . In the second step, we only need to solve a battery replacement problem of ESSs for each bus depot. This battery replacement problem of ESSs can be solved efficiently using DP.

#### 4.4. Heuristics

Although the sub-problems in the LR framework are solved elabo-

rately, the “curse of dimensionality” of DP still leads to an exponential increase in the computational burden as the number of bus fleets increases. For this reason, a heuristic algorithm is presented to find high-quality solutions to M2 quickly. At the beginning of planning year  $\varphi$ , we have to decide  $z_{f\varphi}^b$  and  $x_{f\varphi}$  for all bus fleets and bus depots. In essence, we need to find a one-to-one matching relationship between bus fleets and bus depots.

This study presents two matching strategies illustrated in Fig. 3(a). First, bus fleets are listed in descending order by their SoHs. A “descending” strategy in this context refers to bus depots listed in descending order by their total charging demands matched to the ordered bus fleet list. An “Ascending” strategy in this context refers to bus depots listed in ascending order by their total charging demands matched to the ordered bus fleet list. Finally, we propose a strategy-based DP illustrated in Fig. 3(b). In Fig. 3, we use blue squares to represent the “Descending” strategy and red squares to represent the “ascending” strategy. The decision variable is the strategy chosen at each stage. The state variable is a vector of SoH of bus fleets. After choosing a strategy, we solve a charging scheduling problem associated with constraints (26)–(31) and objective  $\sum_m D_m \sum_t (\delta_{gr} + \lambda_t) g_{f\varphi}$  for each bus fleet. The variable  $z_{f\varphi}^b$  would be set to 1 if the charging scheduling problem is infeasible.

Fig. 4 presents a flowchart of the solution approaches for M2 and M3. The strategy-based DP is used to find a near-optimal solution to a

**Table 1**  
Parameter settings of bus depots.

No.	Number of chargers	Initial capacity of ESS (kWh)	Number of PV modules
1	25	500	613
2	25	300	245
3	20	300	307
4	20	200	245
5	20	200	245
6	15	200	184
7	15	300	307
8	15	300	307
9	20	300	307
10	20	200	245
11	20	500	307
12	15	300	245
13	15	300	245
14	15	200	184
15	20	200	307

**Table 2**  
Electricity prices of public power grids.

Time	Price (US\$/kWh)
0:00–06:00	0.2
06:00–09:00	0.3
09:00–14:00	0.5
14:00–17:00	0.3
17:00–21:00	0.5
21:00–24:00	0.3

subproblem in the LR framework. The solution may not be optimal even though the termination condition is satisfied due to the loss of the optimality for solving subproblems using strategy-based DP. Therefore, computational experiments in Section 5 evaluate the solution efficiency of strategy-based DP. After solving M2, we save the optimal solution to M2 and solve the storage battery replacement problem by considering solar PV energy scheduling. This storage battery replacement problem can also be reformulated as a DP model.

**5. Computational experiments**

This section presents the numerical instances scaled from 2 to 15 bus fleets to evaluate the proposed algorithms and models. Then, a case study is constructed using transit network data and bus operational data in Beijing, China. All instances and the case study are run on a desktop computer with an Intel Core i7-9700K CPU @ 3.60 GHz and 32 GB of memory.

**Table 3**  
Solution time and objective value of M1 and M2.

Ins	M1		M2			M2 <sup>h</sup>		
	Time	Obj	Time	Obj	Gap	Time	Obj	Gap
I2	4.3	16,829,000	9,433	16,693,000	<0.0001	5,120	16,693,000	<0.0001
I3	8.4	23,161,000	587	22,996,000	<0.0001	5,477	23,015,000	0.0008
I4	14	32,656,000	2,238	32,292,000	<0.0001	3,630	32,330,000	0.0013
I5	16	39,968,000	10,000	39,594,000	0.0005	6,564	39,627,000	0.0014
I6	12	47,964,796	10,000	47,593,000	0.001	4,038	47,638,000	0.002
I7	6	55,220,000	10,000	54,994,000	0.0093	8,436	54,889,000	0.0074
I8	8	61,536,000	10,000	61,311,000	0.0165	5,291	61,193,000	0.0146
I9	10	68,801,000	17,000	68,801,000	0.0445	16,725	68,449,000	0.0392
I10	9	76,843,000	10,000	76,611,000	0.0196	7,471	76,494,000	0.0181
I11	36	84,128,000	14,093	84,128,000	0.0466	10,684	83,773,000	0.0422
I12	145	90,688,000	26,545	90,688,000	0.0586	25,462	90,327,000	0.0544
I13	210	100,180,000	15,567	100,180,000	0.079	14,038	99,679,000	0.0737
I14	265	106,510,000	14,330	106,510,000	0.0932	11,967	105,990,000	0.0879
I15	319	114,090,000	14,565	114,090,000	0.1018	12,051	113,580,000	0.0968

<sup>h</sup> Solved with heuristics. The unit of “Time” is second. The unit of “Obj” is US\$. “Ins” represents the numerical instance.

**Table 4**  
Solution time and objective values of M3 using LR and two-step approach.

Instance	Time <sup>†</sup> (s)	Obj <sup>‡</sup> (US\$)	Time <sup>†</sup> (s)	Obj <sup>‡</sup> (US\$)
I2	9,605	16,485,386	10,000	16,621,278
I3	775	22,563,445	10,000	22,728,874
I4	2,415	31,652,752	10,000	32,016,421
I5	10,222	38,796,516	12,000	39,170,014
I6	10,182	46,626,692	12,000	46,998,831
I7	8,617	53,744,534	10,000	54,075,341
I8	5,500	59,840,726	10,000	60,183,731
I9	17,054	66,938,714	20,000	67,290,732
I10	7,920	74,815,739	10,000	75,164,558
I11	11,064	81,916,133	12,000	82,271,116
I12	25,801	88,262,497	26,000	88,623,273
I13	14,325	97,389,509	15,000	97,891,097
I14	12,368	103,493,713	15,000	104,013,498
I15	12,405	110,925,431	15,000	111,435,148

<sup>†</sup> Two-step approach.

<sup>‡</sup> LR.

**5.1. Evaluation of solution approaches and models**

Let the capacity of power batteries for all BEBs be 200 kWh. The price of purchasing a new BEB battery with a capacity of 200 kWh is US\$ 30,000 (Hensher et al., 2022). The recycling price of 1 kWh of retired BEB batteries is US\$ 75/kWh (Lai et al., 2021). The price of 1 kWh of echelon utilization batteries should be higher than US\$ 75/kWh, thereby letting the value be US\$ 90/kWh for numerical instances. We assume that the surplus value of a retired echelon utilization battery is zero. Hence, the recycling price of 1 kWh of echelon utilization batteries is US\$ 0/kWh. The planning horizon is ten years in this study. The average power fading rate of PV modules is 0.5% each year (Wijeratne et al., 2022). The number of chargers, the initial capacity of ESS, and the number of PV modules at bus depots are presented in Table 1. Let the fleet size be 95 for all bus fleets. The energy consumption rate is 0.37 kWh/km (Ma et al., 2021). Electricity prices are listed in Table 2. The price of PV electricity energy recycling is US\$ 0.1/kWh across all hours of day. Let  $\eta_{min}$  be 20%. Let  $\delta_{pv}$  be 0.0008 and  $\delta_{gr}$  be 0.008 (Keyhani, 2014; Liu et al., 2023b). The charging power of chargers is set to 200 kW. Power outputs of PV modules can be obtained using weather and solar irradiance data (Chandra Mouli et al., 2016). Let the parameters of the battery capacity fading model  $\gamma_1, \gamma_2, \gamma_3$ , and  $\gamma_4$  be  $-4.09 \times 10^{-4}$ ,  $-2.17 \times 10^{-5}$ , and 6.13, respectively (Zhang et al., 2021).

Numerical instances scaled from 2 to 15 bus fleets are implemented to examine the proposed solution approaches to M1 and M2. Table 3 presents the solution time and objective function values of M1 and M2. M1 is solved using DP, while M2 is solved using LR and heuristics. The column “Time” records the solution time of instances. The objective

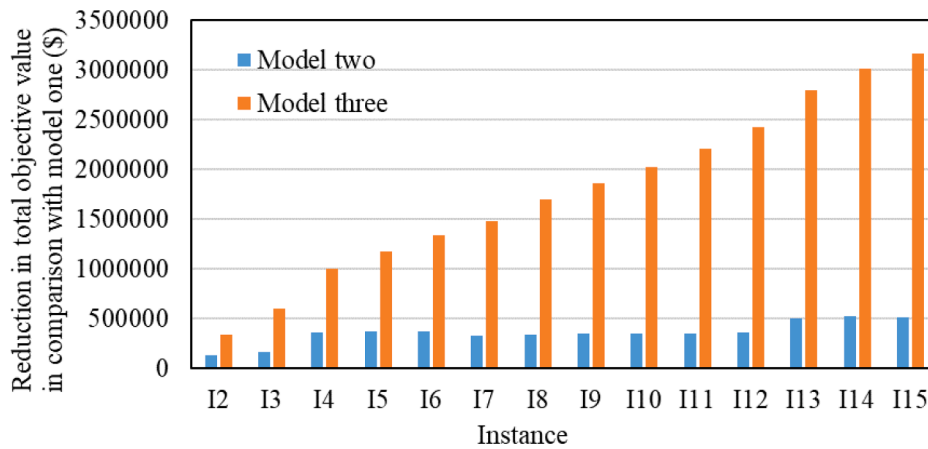


Fig. 5. Reduction in the objective value of M2 and M3 in comparison with M1.

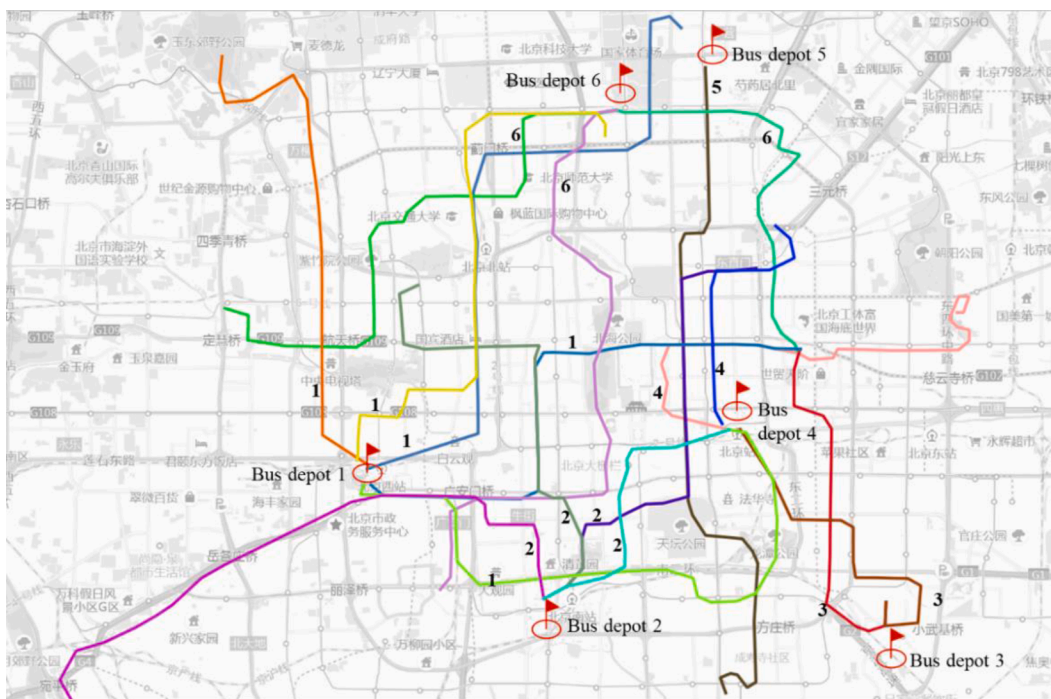


Fig. 6. Bus network layout of the case study.

values of instances are presented in the column “Obj.” In distinguishing LR, we use “M2<sup>h</sup>” to represent M2 solved using heuristics. The column “Gap” measures the gaps between the best upper bounds and the best lower bounds on objective functions of M2 and “M2<sup>h</sup>,” respectively. Notably, the best lower bounds in “M2” and “M2<sup>h</sup>” are provided by LR. The results of M1 indicate that DP can effectively solve a pure battery replacement problem for a single bus fleet. LR provides exact solutions to M2 within acceptable solution time when bus fleets are fewer than seven. However, LR integrated with strategy-based DP performs better than LR in terms of solution efficiency of M2 when the number of bus fleets is not less than seven. The major reason is that the action space of  $x_{fwp}$  in a sub-problem increases rapidly as the number of bus fleets increases when LR is employed.

The same instances are performed to compare LR and the two-step approach for M3. Table 4 presents the solution time and objective values of M3 using LR and the two-step approach. The column “Time<sup>l</sup>” records the CPU time of LR for all instances, while the solution time of the two-step approach is presented in the column “Time<sup>t</sup>.” The columns

“Obj<sup>h</sup>” and “Obj<sup>l</sup>” record the objective values of M3 solved by the two-step approach and LR, respectively. When bus fleets are fewer than seven, LR is employed in the first step of the two-step approach. Strategy-based DP is used in the first step of the two-step approach when the number of bus fleets is not less than seven. The results in Table 4 reveal that the two-step approach performs better than LR in terms of solution efficiency of M3.

Fig. 5 shows the reduction in the objective values of M2 and M3 compared with M1. Taking I13 as an example, compared with the objective value of M1, the objective values of M2 and M3 are reduced by US\$ 510,000 (accounting for 0.45% of the objective value in M1) and US \$ 2,654,852 (accounting for 2.33% of the objective value in M1), respectively. In M2, power battery matching induces a reduction in objective value. In M3, besides power battery matching, deploying PESS also reduces objective value because part of the charging demand of BEBs is satisfied by the electric energy produced by PV power generation infrastructure.

**Table 5**  
Departure frequencies of BEBs at bus depots.

Time	Depot 1	Depot 2	Depot 3	Depot 4	Depot 5	Depot 6
5:00–6:00	26	14	25	0	2	2
6:00–7:00	53	29	33	18	13	19
7:00–8:00	53	44	52	20	15	48
8:00–9:00	74	41	56	28	6	48
9:00–10:00	63	43	54	18	14	48
10:00–11:00	71	48	54	45	7	46
11:00–12:00	65	36	50	10	15	40
12:00–13:00	73	31	60	3	13	40
13:00–14:00	80	45	44	15	12	26
14:00–15:00	54	43	69	30	15	44
15:00–16:00	59	41	54	20	13	35
16:00–17:00	65	41	52	25	17	33
17:00–18:00	54	46	40	40	13	44
18:00–19:00	41	35	46	25	10	34
19:00–20:00	44	28	50	23	6	24
20:00–21:00	21	21	10	18	7	20
21:00–22:00	11	19	13	13	11	9
22:00–23:00	8	6	6	5	2	6
23:00–24:00	0	0	0	0	0	0
0:00–1:00	0	0	0	0	0	0
1:00–2:00	0	0	0	0	0	0
2:00–3:00	0	0	0	0	0	0
3:00–4:00	0	0	0	0	0	0
4:00–5:00	0	0	0	0	0	0

**Table 6**  
Original depot-fleet matching information obtained from real-word operation data.

Bus depot No.	Bus fleet No.	Fleet size	Initial power battery capacity (kWh)
1	1	160	200
2	2	95	200
3	3	83	200
4	4	36	200
5	5	36	200
6	6	95	200

5.2. Case study

This case study focuses on a bus network encompassing six bus depots and 17 bus routes in Beijing, China. The layout of the bus network is illustrated in Fig. 6, where the numbers marked beside bus lines represent the corresponding bus depots. We assume that six bus fleets are exactly used to match six bus depots for serving passengers along bus routes. Smart card data of customers and bus GPS trajectories are utilized to estimate the departure time of BEBs at bus depots. The departure frequencies of BEBs at bus depots are presented in Table 5. The travel time is obtained by calling AMAP (<https://www.amap.com/>). The other parameters are the same as those in Section 5.1. Original depot-fleet matching information obtained from real-world operation data is presented in Table 6. The solution time for solving M1 is nine seconds, while 16,533 and 18,674 seconds are taken to solve M2 and M3, respectively.

The results of power battery matching, power battery replacement for BEBs, and battery replacement for ESSs in M3 are illustrated in Fig. 7. In this case study, no bus fleet needs to replace new power batteries during the entire planning horizon; therefore, the battery replacement for bus fleets are not shown in Fig. 7. For bus fleets 1 and 3, buses (power batteries) are assigned to bus depots 1 and 3, respectively, during the entire planning horizon. Other bus fleets are assigned to different bus depots at different years. For example, bus fleet 2 is assigned to bus depots as the sequence of (2,6,6,2,2,2,2,2,6) shows. Bus fleets 2 and 6 have the same fleet size, and both bus fleets 2 and 6 can serve bus depots 2 and 6. Therefore, the sequence of (2,6,6,2,2,2,2,2,6) only includes the elements of “2” and “6.” The results of battery replacement for ESSs are also presented in Fig. 7. For instance, batteries of ESSs at bus depot 6 are replaced only once during the entire planning horizon.

The total cost in M1 is US\$ 49,218,000. The solution to M1 indicates no need for any bus fleet to replace batteries within the planning horizon. The reason is that the predetermined capacity of BEB batteries is sufficient to support ten years under the battery capacity fading model used in the case study. The charging cost of BEBs is reduced by US\$ 222,528 when power battery replacement and matching (M2) are optimized jointly. The changes in the battery capacity of bus fleets 2, 6, 4, and 5 for M1 and M2 are shown in Fig. 8. The changes in the battery capacity of bus fleets 1 and 3 are not presented because the fading trends of battery capacity in M1 and M2 are the same. The findings indicate that not all bus fleets benefit from the bus fleet reallocation, e.g., bus

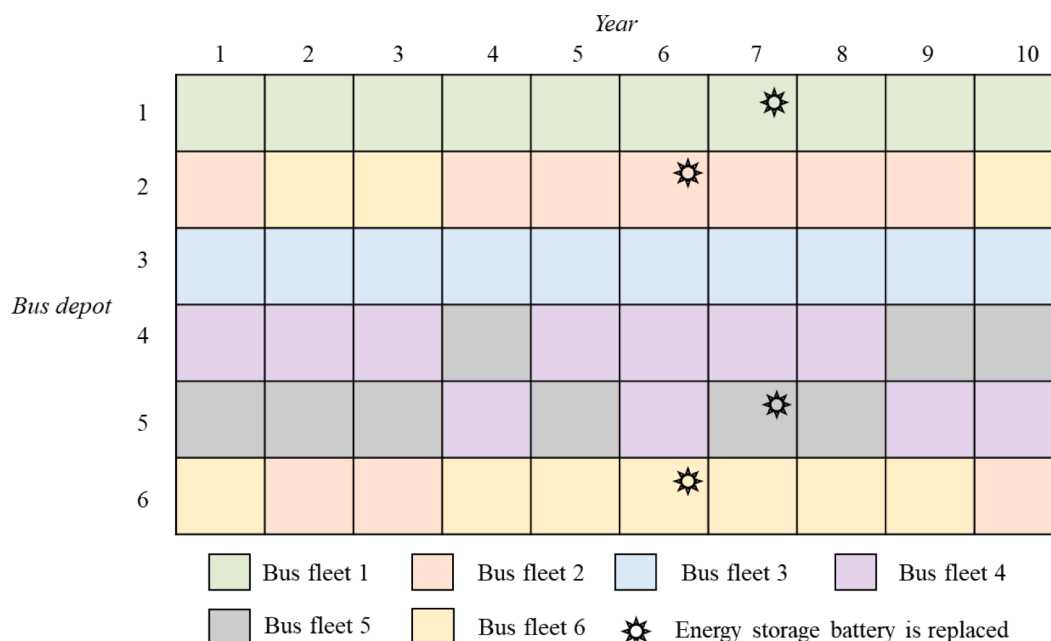


**Fig. 7.** Results of power battery matching, battery replacement for BEBs, and battery replacement for ESSs.

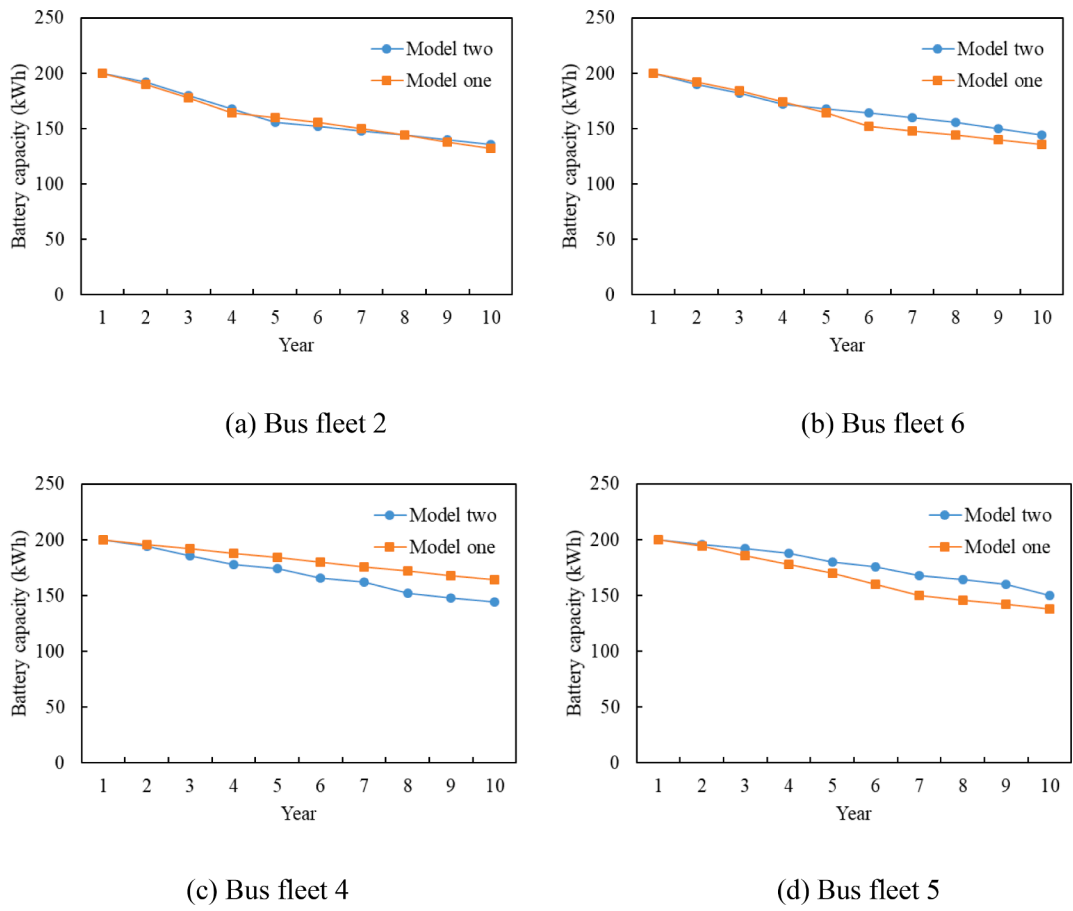


Fig. 8. Changes in battery capacity of bus fleets 2, 6, 4, and 5 for M1 and M2.

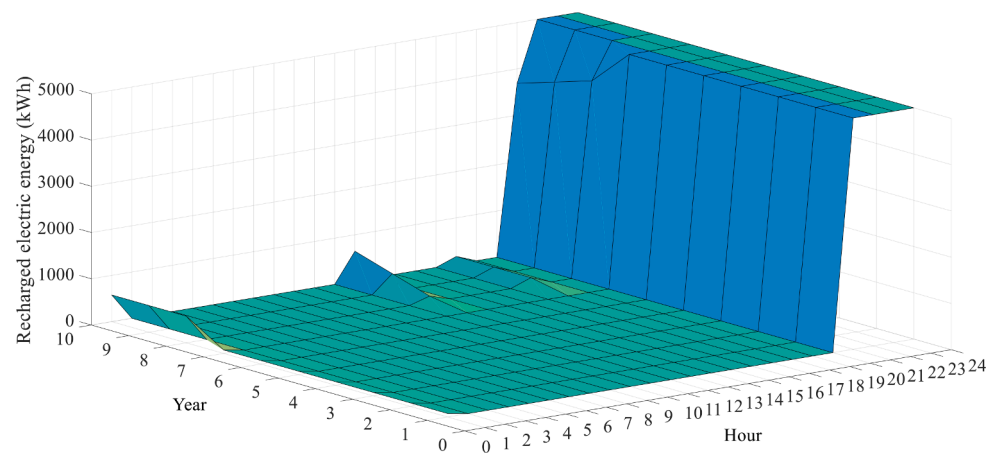


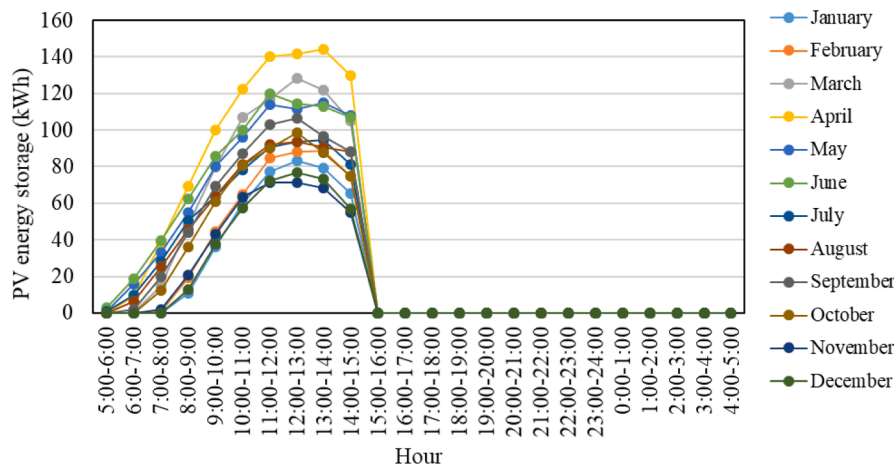
Fig. 9. Charging schedules of bus fleet 1 during the entire planning horizon.

fleet 4. Naturally, the charging cost of bus fleet 4 increases, but the total charging cost of six bus fleets has dropped by US\$ 222,528. Notably, our results of changes in the battery capacity of different bus fleets are similar to the study implemented by Wang et al. (2020). System optimization sometimes has to sacrifice individual bus fleets to minimize total system costs.

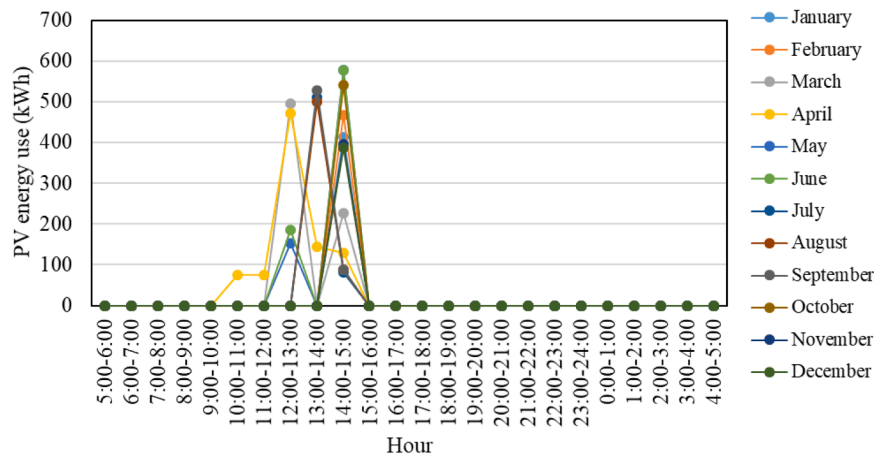
Compared with M1, the total cost in M3 is reduced by US\$ 1,366,955. In M3, the reduction in charging and carbon emission costs is induced because of PESS. When part of the charging demand of BEBs is satisfied by PV power generation infrastructure, the corresponding carbon emission produced by coal-fired power generation is also

reduced. The number of BEBs in the case study is 505, indicating that the cost reduction per bus yearly is approximately US\$ 271 in M3.

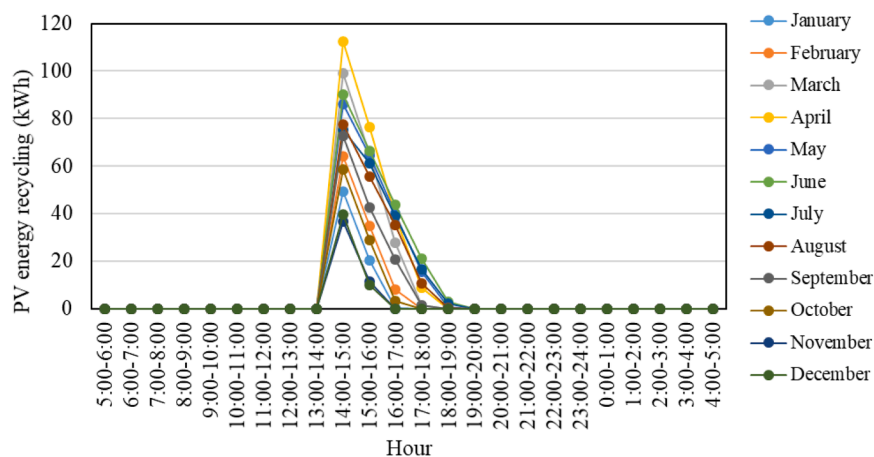
The total recharged electric energy of bus fleet  $f$  at hour  $t$  and year  $\varphi$  is a crucial decision variable to respond to the time-of-use tariffs. As the battery capacity fades in a bus fleet, the change in the charging schedule should be understood well. Fig. 9 also shows that the charging schedule changes in the 8th year of the planning horizon. The results of M3 indicate that bus fleet 1 is assigned to bus depot 1 during the entire planning horizon. Hence, the total energy consumption of a day is constant over the years for bus fleet 1, but the battery capacity fades over the years. Fig. 9 also shows that the charging schedule does not



(a) Solar PV energy storage



(b) Solar PV energy use



(c) Solar PV energy recycling

Fig. 10. Solar PV energy storage, use, and recycling at bus depot 1 in the first year of the planning horizon.

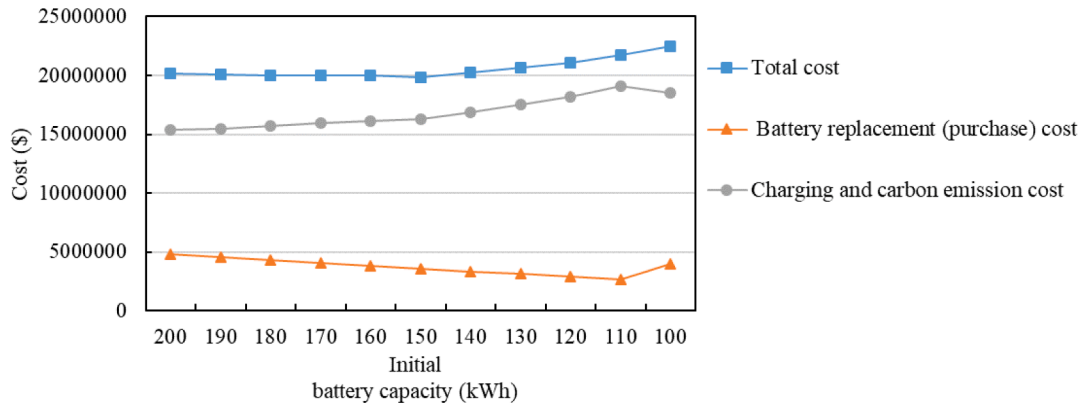


Fig. 11. Cost profiles in M1 for bus fleet 1 as the capacity of new batteries changes.

change until the 8th year. In the first seven years, BEBs are recharged in the last four hours (1:00–5:00) when the electricity price is the lowest (US\$ 0.2/kWh). When the battery capacity fades further, BEBs have to be recharged at periods (17:00–18:00 and 22:00–23:00) with higher electricity prices (US\$ 0.5/kWh and US\$ 0.3/kWh). Our results of the charging demand distributions align with the findings of Liu et al. (2023). The study highlights that as battery capacity fades, BEBs cannot cover all service trips unless some are charged during these higher-price periods.

Solar PV energy scheduling in M3 is vital in reducing charging and carbon emission costs. PV energy scheduling involves PV energy storage, use, and recycling. The electric energy produced by PV power generation facilities is allowed to flow into local ESSs or public grids. PV energy stored in ESSs is used to charge BEBs. PV energy flowing into public grids induces earnings at a real-time price of PV electricity energy recycling. For example, Fig. 10 shows PV energy storage, use, and recycling at bus depot 1 in the first year of the planning horizon. As shown in Fig. 10(a), PV energy is stored from 5:00–16:00 for all months. PV energy does not flow into ESS anymore after 16:00 due to the capacity limit of ESS. Fig. 10(b) indicates that energy use varies depending on PV power outputs of different months. Fig. 10(c) is easy to understand because PV energy must flow into public grids due to the capacity limit.

The capacity of new batteries of BEBs is a crucial design parameter for PT systems. Given the sizes of fleets, transit agencies should find an

optimal battery capacity for BEBs to minimize the sum of battery replacement (purchase) cost, charging cost, and carbon emission cost. To investigate this issue, we take bus fleet 1 as an example. The sensitivity analysis of the capacity of new batteries is performed by solving M1. In the first year of the planning horizon, the battery purchase cost of bus fleet 1 is also added to the total cost. Fig. 11 presents the cost profiles in M1 for bus fleet 1 as initial battery capacity changes. The optimal initial battery capacity equals 150 kWh for bus fleet 1. The battery replacement (purchase) cost linearly drops as the initial battery capacity decreases, except when the initial battery capacity reaches 100 kWh. Batteries of bus fleet 1 have to be replaced by new batteries when the new battery capacity reaches 100 kWh. The nonlinear downward trend of charging and carbon emission cost is presented in Fig. 11 as the capacity of new batteries decreases. Similar experiment processes are performed for bus fleets 2, 3, 4, 5, and 6. The optimal capacities of new batteries for bus fleets 2, 3, 4, 5, and 6 are 170, 150, 120, 150, and 160 kWh, respectively. Similar to the findings from the research by He et al. (2019), the results suggest that the optimal capacities of new batteries for bus fleets depend on the characteristics of bus fleets and the corresponding bus depots (working load).

As energy storage units, echelon utilization batteries are deployed with PV power generation facilities at bus depots. The sensitivity analysis of the price of echelon utilization batteries (PEUB) is performed by taking the example of bus fleet 3 and bus depot 3. The PEUB ranges from US\$ 80/kWh to US\$ 100/kWh. The results from M3 indicate echelon

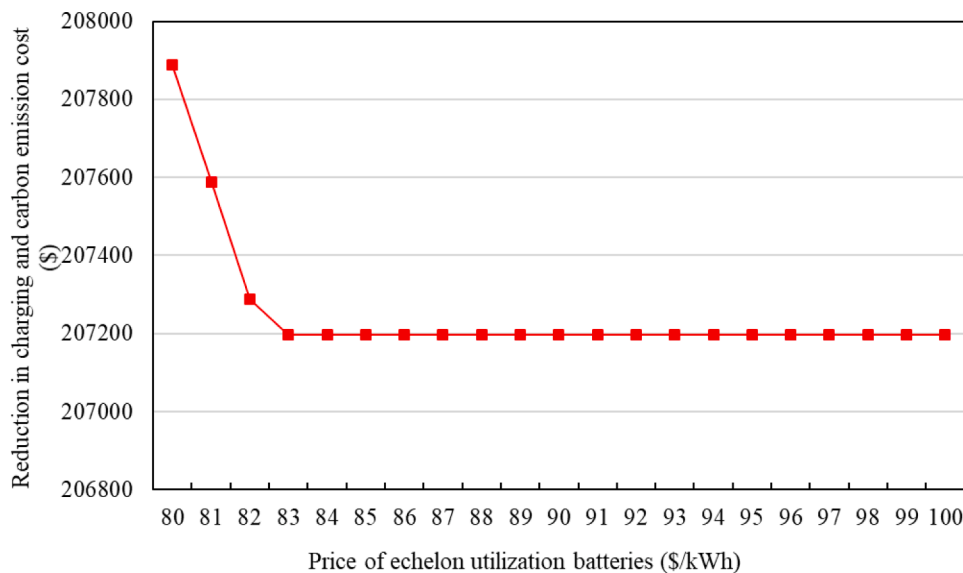


Fig. 12. Reduction in charging and carbon costs of bus fleet 3 and bus depot 3 in M3 as the price of echelon utilization batteries changes.

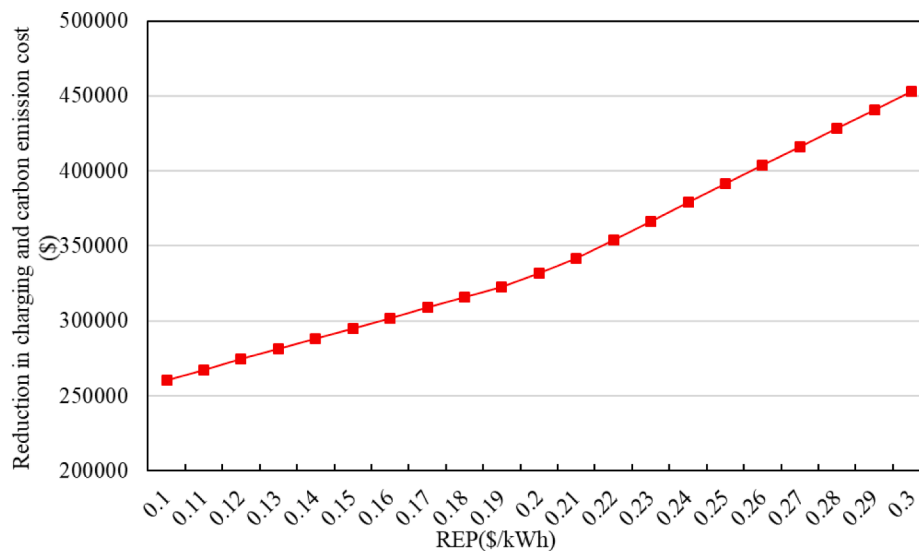


Fig. 13. Reduction in charging and carbon costs of bus fleet 3 and bus depot 3 in M3 as the recycling electricity price changes.

utilization batteries for PESS are replaced only in the third year of the planning horizon when PEUB ranges from US\$ 80/kWh to US\$ 82/kWh. As PEUB increases from US\$ 83/kWh to US\$ 100/kWh, echelon utilization batteries need not be replaced during the entire planning horizon. Compared with M2, the charging and carbon cost reduction of bus fleet 3 and bus depot 3 in M3 is also shown in Fig. 12. The charging and carbon cost reduction is reduced by US\$ 691 as PEUB rises from US\$ 80/kWh to US\$ 100/kWh. Hence, the impact of PEUB on the objective value of M3 is small.

The sensitivity analysis of recycling electricity price (REP) of PV power generation is conducted using the example of bus fleet 3 and bus depot 3. REP is a crucial parameter influencing PV energy scheduling in M3. Let REP rise from US\$ 0.1/kWh to US\$ 0.3/kWh with an increasing step of 0.01. The results of M3 indicate echelon utilization batteries for PESS are replaced only in the sixth year of the planning horizon when REP is smaller than US\$ 0.19/kWh. As REP ranges from US\$ 0.19/kWh to US\$ 0.3/kWh, echelon utilization batteries need not be replaced during the entire planning horizon. Compared with M2, the nonlinear reducing trend of charging and carbon cost of bus fleet 3 and bus depot 3 in M3 is shown in Fig. 13. The reduction in charging and carbon cost is reduced by approximately US\$ 190,000 as REP rises from US\$ 0.1/kWh to US\$ 0.3/kWh. Therefore, the impact of REP on the objective value of M3 is significant.

## 6. Conclusion

This study presents a sustainable battery scheduling and echelon utilization framework for an electric bus network integrated with PESS. A battery capacity fading model is employed to capture the impacts of battery capacity degradation on the daily operations of electric buses. Customized dynamic programming and Lagrange relaxation are developed to solve the nonlinear optimization models. A case study is constructed using data from the transit network and bus operations in Beijing, China. The case study examines the solution characteristics of the three proposed models, aiming to evaluate their performance and offer valuable managerial insights. The sensitivity analysis of the initial battery capacity (actual battery capacity at the beginning of the planning horizon) of electric buses indicates the nonlinear downward trend of charging and carbon emission cost as initial battery capacity

decreases. The sensitivity analysis of the price of echelon utilization batteries reveals its minimal impact on the total cost. The sensitivity analysis of the price of PV recycling electricity shows that it significantly influences the recharging and carbon emission costs. The results show how the sustainable battery scheduling and echelon utilization framework impacts the electric bus systems. The study findings could also provide insights for transit agencies to promote clean, green, and sustainable operation modes.

The smart power grid, public grid, PESS, and transit network will be jointly considered using optimization approaches in future investigations. The uncertainty factors in the models, such as climate change, battery costs, and transportation network speed (Ma et al., 2020), should also be considered from a sustainable perspective in future research.

## CRedit authorship contribution statement

**Xiaohan Liu:** Formal analysis, Methodology, Writing – original draft. **Wen-Long Shang:** Resources, Writing – review & editing. **Gonçalo Homem de Almeida Correia:** Formal analysis, Investigation, Validation, Writing – review & editing. **Zhengke Liu:** Data curation, Investigation. **Xiaolei Ma:** Conceptualization, Formal analysis, Funding acquisition, Supervision, Writing – review & editing.

## Declaration of Competing Interest

The authors declare that they have no known competing financial interests or personal relationships that could have appeared to influence the work reported in this paper.

## Data availability

Data will be made available on request.

## Acknowledgements

This study was funded by Beijing Nova Program (20230484432).

Supplementary materials

Supplementary material associated with this article can be found, in the online version, at [doi:10.1016/j.scs.2023.105108](https://doi.org/10.1016/j.scs.2023.105108).

Appendix A

Table A1

Table A1

Notations of indices, sets, parameters, and variables used in this study.

Indices	
$\varphi$	Index of year in a plan
$m$	Index of month in a year
$t$	Index of hour in a day
$f$	Index of bus fleets
$w$	Index of bus depots
$r$	Index of bus routes
Sets	
$\Gamma = (1, \dots, \varphi, \dots)$	Set of years in a planning horizon
$M = (1, \dots, m, \dots)$	Set of months in a year
$T = (1, \dots, t, \dots)$	Set of hours in a day
$F = (1, \dots, f, \dots)$	Set of bus fleets
$W = (1, \dots, w, \dots)$	Set of bus depots
$R_w = (1, \dots, r, \dots)$	Set of bus routes associated with bus depot $w$
Parameters	
$\alpha_1$	Price of purchasing a power battery with a certain capacity (US\$)
$\alpha_2$	Recycling price of 1 kWh of retired power batteries (US\$/kWh)
$\alpha_3$	Price of 1 kWh of echelon utilization batteries (US\$/kWh)
$\alpha_4$	Recycling price of 1 kWh of echelon utilization batteries (US\$/kWh)
$o_\varphi$	Power fading rate of photovoltaic modules at year $\varphi$
$N_f$	Size of bus fleet $f$
$\bar{y}_{r,t}$	Number of service trips at hour $t$ for bus route $r$
$t_r$	Travel time of a round-trip for bus route $r$ (h)
$e_r$	Energy consumption of an electric bus driving along route $r$ (kWh)
$\bar{E}_f$	Initial battery capacity of a bus in fleet $f$ (kWh)
$\bar{C}_w$	Initial capacity of energy storage system at bus depot $w$ (kWh)
$\eta_{\min}$	Minimum state of charge
$D_m$	Number of days in month $m$
$\delta_{pv}$	Carbon emission cost of 1 kWh of electricity produced via photovoltaic power generation (US\$/kWh)
$\delta_{gr}$	Carbon emission cost of 1 kWh of electricity produced by coal-fired power plants (US\$/kWh)
$\lambda_t$	Electricity price at hour $t$ (US\$/kWh)
$\lambda'_t$	Price of photovoltaic electricity energy recycling at hour $t$ (US\$/kWh)
$A_w$	Number of photovoltaic modules installed at bus depot $w$
$c_w$	Number of chargers installed at bus depot $w$
$P_{gr}$	Charging power of chargers (kW)
$P_{mt}$	Power output of the photovoltaic module at hour $t$ and month $m$ (kW)
Decision variables	
$z_{f\varphi}^b$	1 if the transit agency purchases new power batteries for bus fleet $f$ at the beginning of year $\varphi$ and 0 otherwise
$z_{w\varphi}^s$	1 if the transit agency purchases echelon utilization batteries for energy storage of bus depot $w$ at the beginning of year $\varphi$ and 0 otherwise
$x_{fw\varphi}$	1 if power batteries of bus fleet $f$ are reallocated to bus depot $w$ at the beginning of year $\varphi$ and 0 otherwise
$E_{f\varphi}$	Current power battery capacity of a vehicle associated with bus fleet $f$ at the end of year $\varphi$ (kWh)
$E'_{f\varphi}$	Current power battery capacity of a vehicle associated with bus fleet $f$ after the decision of battery replacement is made at the beginning of year $\varphi$ (kWh)
$C_{w\varphi}$	Current total capacity of energy storage of bus depot $w$ at the end of year $\varphi$ (kWh)
$C'_{w\varphi}$	Current total capacity of energy storage of bus depot $w$ after the decision of battery replacement is made at the beginning of year $\varphi$ (kWh)
$g_{ft\varphi}$	Total recharged electric energy of bus fleet $f$ at hour $t$ and year $\varphi$ (kWh)
$h_{ft\varphi}$	Total layover time of bus fleet $f$ at hour $t$ and year $\varphi$ (h)
$h_{ft\varphi}$	Total recharging time of bus fleet $f$ at hour $t$ and year $\varphi$ (h)
$z_{f\varphi}^{sb}$	Amount of reduced power battery capacity of a vehicle associated with bus fleet $f$ at year $\varphi$ (kWh)
$z_{w\varphi}^{ss}$	Amount of reduced energy storage capacity of bus depot $w$ at year $\varphi$ (kWh)
$u_{mtw\varphi}$	Amount of photovoltaic electricity released from energy storage for charging at bus depot $w$ at hour $t$ in month $m$ of year $\varphi$ (kWh)
$v_{mtw\varphi}$	Amount of photovoltaic electricity flowing into energy storage for charging at bus depot $w$ at hour $t$ in month $m$ of year $\varphi$ (kWh)

References

Bashash, S., Moura, S. J., Forman, J. C., & Fathy, H. K. (2011). Plug-in hybrid electric vehicle charge pattern optimization for energy cost and battery longevity. *Journal of Power Sources*, 196(1), 541–549. <https://doi.org/10.1016/j.jpowsour.2010.07.001>

Calise, F., Fabozzi, S., Vanoli, L., & Vicidomini, M. (2021). A sustainable mobility strategy based on electric vehicles and photovoltaic panels for shopping centers.

*Sustainable Cities and Society*, 70, Article 102891. <https://doi.org/10.1016/j.scs.2021.102891>

Mouli, Chandra, R. G., Bauer, P., & Zeman, M. (2016). System design for a solar powered electric vehicle charging station for workplaces. *Applied Energy*, 168, 434–443. <https://doi.org/10.1016/j.apenergy.2016.01.110>

Cui, S., Xue, Y., Gao, K., Lv, M., & Yu, B. (2023). Adaptive collision-free trajectory tracking control for string stable bidirectional platoons. *IEEE Transactions on*

- Intelligent Transportation Systems*, 1–13. <https://doi.org/10.1109/TITS.2023.3286587>
- Borray, Felipe Cortés, Garcés, A., Merino, A., Torres, E., & Mazón, J. (2021). New energy bound-based model for optimal charging of electric vehicles with solar photovoltaic considering low-voltage network's constraints. *International Journal of Electrical Power & Energy Systems*, 129, Article 106862. <https://doi.org/10.1016/j.ijepes.2021.106862>
- Low or no emission vehicle program - 5339(c). (2022). Federal Transit Administration. Retrieved from <https://www.transit.dot.gov/lowno> Accessed January 19, 2023.
- Han, S., Han, S., & Aki, H. (2014). A practical battery wear model for electric vehicle charging applications. *Applied Energy*, 113, 1100–1108. <https://doi.org/10.1016/j.apenergy.2013.08.062>
- He, Y., Song, Z., & Liu, Z. (2019). Fast-charging station deployment for battery electric bus systems considering electricity demand charges. *Sustainable Cities and Society*, 48, Article 101530. <https://doi.org/10.1016/j.scs.2019.101530>
- Hensher, D. A., Wei, E., & Balbontin, C. (2022). Comparative assessment of zero emission electric and hydrogen buses in Australia. *Transportation Research Part D: Transport and Environment*, 102, Article 103130. <https://doi.org/10.1016/j.trd.2021.103130>
- International Energy Agency. (2022). *Transport: Sectoral overview*. Retrieved from <https://www.iea.org/reports/transport> Accessed July 11, 2022.
- International Energy Agency. (2023). *Cars and vans*. Retrieved from <https://www.iea.org/energy-system/transport/cars-and-vans> Accessed July 11, 2022.
- Jirdehi, M. A., & Tabar, V. S. (2023). Multi-objective long-term expansion planning of electric vehicle infrastructures integrated with wind and solar units under the uncertain environment considering demand side management: A real test case. *Sustainable Cities and Society*, 96, Article 104632. <https://doi.org/10.1016/j.scs.2023.104632>
- Keyhani, A. (2014). *Design of Smart Power Grid Renewable Energy Systems* (2nd Edition).
- Koten, H., & Bilal, S. (2018). Recent developments in electric vehicles. *International Journal of Advances on Automotive and Technology*, 1(1), 35–52. <https://doi.org/10.15659/ijaat.18.01.890>
- Koten, H. (2018). Hybrid and electric vehicles for Istanbul cycle and drivetrain design. *Sigma*, 9(4), 461–470.
- Lai, X., Huang, Y., Deng, C., Gu, H., Han, X., Zheng, Y., & Ouyang, M. (2021). Sorting, regrouping, and echelon utilization of the large-scale retired lithium batteries: A critical review. *Renewable and Sustainable Energy Reviews*, 146, Article 111162. <https://doi.org/10.1016/j.rser.2021.111162>
- Lam, L., & Bauer, P. (2013). Practical capacity fading model for Li-ion battery cells in electric vehicles. *IEEE Transactions on Power Electronics*, 28(12), 5910–5918. <https://doi.org/10.1109/TPEL.2012.2235083>
- Liu, X., Qu, X., & Ma, X. (2021). Optimizing electric bus charging infrastructure considering power matching and seasonality. *Transportation Research Part D: Transport and Environment*, 100, Article 103057. <https://doi.org/10.1016/j.trd.2021.103057>
- Liu, X., Liu, X. C., Zhang, X., Zhou, Y., Chen, J., & Ma, X. (2022). Optimal location planning of electric bus charging stations with integrated photovoltaic and energy storage system. *Computer-Aided Civil and Infrastructure Engineering*, 38, 1424–1446. <https://doi.org/10.1111/micc.12935>
- Liu, X., Liu, X. C., Xie, C., & Ma, X. (2023a). Impacts of photovoltaic and energy storage system adoption on public transport: A simulation-based optimization approach. *Renewable and Sustainable Energy Reviews*, 181, Article 113319. <https://doi.org/10.1016/j.rser.2023.113319>
- Liu, X., Liu, X. C., Liu, Z., Shi, R., & Ma, X. (2023b). A solar-powered bus charging infrastructure location problem under charging service degradation. *Transportation Research Part D: Transport and Environment*, 119, Article 103770. <https://doi.org/10.1016/j.trd.2023.103770>
- Lopez De Briñas Gorosabel, O., Xylia, M., & Silveira, S. (2022). A framework for the assessment of electric bus charging station construction: A case study for Stockholm's inner city. *Sustainable Cities and Society*, 78, Article 103610. <https://doi.org/10.1016/j.scs.2021.103610>
- Majumder, S., De, K., Kumar, P., & Rayudu, R. (2019). A green public transportation system using E-buses: A technical and commercial feasibility study. *Sustainable Cities and Society*, 51, Article 101789. <https://doi.org/10.1016/j.scs.2019.101789>
- Ma, X., Zhong, H., Li, Y., Ma, J., Cui, Z., & Wang, Y. (2020). Forecasting transportation network speed using deep capsule networks with nested LSTM models. *IEEE Transactions on Intelligent Transportation Systems*, 22(8), 4813–4824. <https://doi.org/10.1109/TITS.2020.2984813>
- Ma, X., Miao, R., Wu, X., & Liu, X. (2021). Examining influential factors on the energy consumption of electric and diesel buses: A data-driven analysis of large-scale public transit network in Beijing. *Energy*, 216, Article 119196. <https://doi.org/10.1016/j.energy.2020.119196>
- Pelletier, S., Jabali, O., Mendoza, J. E., & Laporte, G. (2019). The electric bus fleet transition problem. *Transportation Research Part C: Emerging Technologies*, 109, 174–193. <https://doi.org/10.1016/j.trc.2019.10.012>
- Perumal, S. S. G., Lusby, R. M., & Larsen, J. (2022). Electric bus planning & scheduling: A review of related problems and methodologies. *European Journal of Operational Research*, 301(2), 395–413. <https://doi.org/10.1016/j.ejor.2021.10.058>
- Peterson, S. B., Apt, J., & Whitacre, J. F. (2010). Lithium-ion battery cell degradation resulting from realistic vehicle and vehicle-to-grid utilization. *Journal of Power Sources*, 195(8), 2385–2392. <https://doi.org/10.1016/j.jpowsour.2009.10.010>
- Powell, W. B. (2010). What you should know about approximate dynamic programming. *Naval Research Logistics*, 56, 239–249. <https://doi.org/10.1002/nav.20347>
- Ramadhani, U. H., Fachrizal, R., Shepero, M., Munkhammar, J., & Widén, J. (2021). Probabilistic load flow analysis of electric vehicle smart charging in unbalanced LV distribution systems with residential photovoltaic generation. *Sustainable Cities and Society*, 72, Article 103043. <https://doi.org/10.1016/j.scs.2021.103043>
- Ren, H., Ma, Z., Ming Lun Fong, A., & Sun, Y. (2022a). Optimal deployment of distributed rooftop photovoltaic systems and batteries for achieving net-zero energy of electric bus transportation in high-density cities. *Applied Energy*, 319, Article 119274. <https://doi.org/10.1016/j.apenergy.2022.119274>
- Ren, H., Ma, Z., Fai Norman Tse, C., & Sun, Y. (2022b). Optimal control of solar-powered electric bus networks with improved renewable energy on-site consumption and reduced grid dependence. *Applied Energy*, 323, Article 119643. <https://doi.org/10.1016/j.apenergy.2022.119643>
- Sathre, R., Scown, C. D., Kavvada, O., & Hendrickson, T. P. (2015). Energy and climate effects of second-life use of electric vehicle batteries in California through 2050. *Journal of Power Sources*, 288, 82–91. <https://doi.org/10.1016/j.jpowsour.2015.04.097>
- Schäfer, A. W., & Yeh, S. (2020). A holistic analysis of passenger travel energy and greenhouse gas intensities. *Nature Sustainability*, 3(6), 459–462. <https://doi.org/10.1038/s41893-020-0514-9>
- Slattery, M., Dunn, J., & Kendall, A. (2021). Transportation of electric vehicle lithium-ion batteries at end-of-life: A literature review. *Resources, Conservation and Recycling*, 174, Article 105755. <https://doi.org/10.1016/j.resconrec.2021.105755>
- Sullivan, W. G., McDonald, T. N., & Van Aken, E. M. (2002). Equipment replacement decisions and lean manufacturing. *Robotics and Computer-Integrated Manufacturing*, 18(3), 255–265. [https://doi.org/10.1016/S0736-5845\(02\)00016-9](https://doi.org/10.1016/S0736-5845(02)00016-9)
- Wang, J., Kang, L., & Liu, Y. (2020). Optimal scheduling for electric bus fleets based on dynamic programming approach by considering battery capacity fade. *Renewable and Sustainable Energy Reviews*, 130, Article 109978. <https://doi.org/10.1016/j.rser.2020.109978>
- Wijeratne, W. M. P. U., Samarasinghalage, T. I., Yang, R. J., & Wakefield, R. (2022). Multi-objective optimisation for building integrated photovoltaics (BIPV) roof projects in early design phase. *Applied Energy*, 309, Article 118476. <https://doi.org/10.1016/j.apenergy.2021.118476>
- Yan, H., Ma, X., & Pu, Z. (2022). Learning dynamic and hierarchical traffic spatiotemporal features with transformer. *IEEE Transactions on Intelligent Transportation Systems*, 23(11), 22386–22399. <https://doi.org/10.1109/TITS.2021.3102983>
- Yang, S., Wang, X., Ning, W., & Jia, X. (2021). An optimization model for charging and discharging battery-exchange buses: Consider carbon emission quota and peak-shaving auxiliary service market. *Sustainable Cities and Society*, 68, Article 102780. <https://doi.org/10.1016/j.scs.2021.102780>
- Zang, Y., Wang, M., & Qi, M. (2022). A column generation tailored to electric vehicle routing problem with nonlinear battery depreciation. *Computers & Operations Research*, 137, Article 105527. <https://doi.org/10.1016/j.cor.2021.105527>
- Zhang, Y., Xiong, R., He, H., Qu, X., & Pecht, M. (2019). State of charge-dependent aging mechanisms in graphite/Li(NiCoAl)O<sub>2</sub> cells: Capacity loss modeling and remaining useful life prediction. *Applied Energy*, 255, Article 113818. <https://doi.org/10.1016/j.apenergy.2019.113818>
- Zhang, L., Zeng, Z., & Qu, X. (2020). On the role of battery capacity fading mechanism in the lifecycle cost of electric bus fleet. *IEEE Transactions on Intelligent Transportation Systems*, 22(4), 2371–2380. <https://doi.org/10.1109/TITS.2020.3014097>
- Zhang, L., Wang, S., & Qu, X. (2021). Optimal electric bus fleet scheduling considering battery degradation and non-linear charging profile. *Transportation Research Part E: Logistics and Transportation Review*, 154, Article 102445. <https://doi.org/10.1016/j.tre.2021.102445>
- Zhang, L., Liu, Z., Wang, W., & Yu, B. (2022). Long-term charging infrastructure deployment and bus fleet transition considering seasonal differences. *Transportation Research Part D: Transport and Environment*, 111, Article 103429. <https://doi.org/10.1016/j.trd.2022.103429>
- Zhou, C., Qian, K., Allan, M., & Zhou, W. (2011). Modeling of the cost of EV battery wear due to V2G application in power systems. *IEEE Transactions on Energy Conversion*, 26(4), 1041–1050. <https://doi.org/10.1109/TEC.2011.2159977>
- Zhou, Y., Liu, X. C., Wei, R., & Golub, A. (2021). Bi-objective optimization for battery electric bus deployment considering cost and environmental equity. *IEEE Transactions on Intelligent Transportation Systems*, 22(4), 2487–2497. <https://doi.org/10.1109/TITS.2020.3043687>